Wada *et al. Biochar* (2026) 8:61
https://doi.org/10.1007/s42773-025-00565-w

Biochar

REVIEW Open Access

# AI-driven biochar engineering for emerging pollutants removal from water: performance, mechanisms, and environmental perspectives

Ojima Z. Wada[1], Gordon McKay[2], Tareq Al-Ansari[1,2] and Khaled A. Mahmoud[1*]

## Abstract

The global prevalence of emerging pollutants (EPs) in aqueous systems presents a significant environmental threat that conventional treatments cannot adequately address. This review provides a comprehensive analysis of biochar-based systems as a sustainable solution, charting a path from foundational material science to advanced, data-driven engineering. We critically evaluate these solutions through a tiered framework: starting with Tier 1 (Pristine Biochar), which is highly reliant on physisorption mechanisms; moving to Tier 2 (Modified Biochar) with enhanced surface properties through activation and/or heteroatom doping; and culminating in Tier 3 (Advanced Composites) incorporating materials like nanoparticles and graphene, which offer superior removal mechanisms, including chemisorption and photocatalysis. A central focus is placed on the transformative role of Artificial Intelligence (AI), which enables predictive modelling and optimization to accelerate the design of tailored, high-performance adsorbents. Beyond performance, this review delves into the critical aspects of scalability, presenting a detailed analysis of the economic trade-offs and environmental/ecotoxicity considerations that govern real-world deployment. We demonstrate how this tiered approach leads to targeted solutions for challenging EPs, such as cationic composites for per- and polyfluoroalkyl substances and engineered surface porosity for the physical entrapment of micro- and nanoplastics. Ultimately, we advocate for an AI-guided strategy, prioritizing sustainable pristine biochar where effective and strategically deploying advanced composites as a last resort. This work concludes by outlining a roadmap for future research, emphasizing the need for standardized and robust datasets, green synthesis protocols, and rigorous safety assessments to ensure the responsible development of these next-generation water treatment technologies.

## Highlights

- Biochar is a highly tunable platform whose engineered forms enable diverse mechanisms for emerging pollutant removal.
- A hybrid machine-learning–driven framework was proposed to guide the process from feedstock selection to selective pollutant removal.
- Despite superior performance, advanced composites face scalability hurdles due to cost and ecotoxicity compared to pristine biochar.

**Keywords** Micropollutants, Resource recovery, AI-Engineering, Nanomaterials, Wastewater treatment, Biomass valorization

*Correspondence:
Khaled A. Mahmoud
kmahmoud@hbku.edu.qa
Full list of author information is available at the end of the article



Springer

**Graphical Abstract**

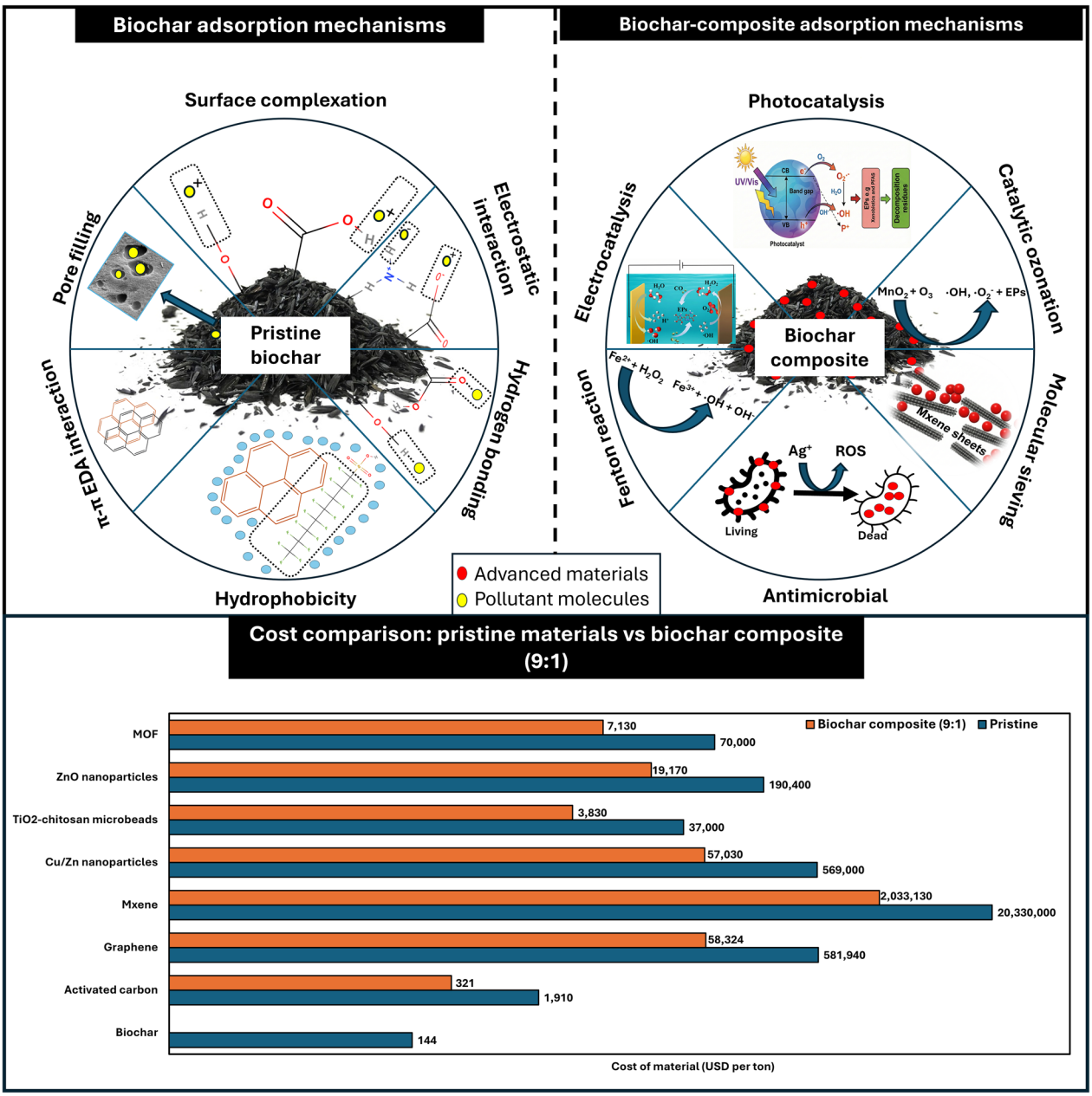


## 1 Introduction

The integrity of global water resources is increasingly compromised by the presence of emerging pollutants (EPs), a diverse and growing class of anthropogenic compounds that pose significant risks to aquatic ecosystems and human health. These substances, including pharmaceuticals and personal care products (PPCPs), persistent organic pollutants (POPs) like per- and polyfluoroalkyl substances (PFAS), pesticides, and engineered nanoparticles (ENPs), are now detected worldwide in surface, ground, and even treated drinking water (Wada and Olawade 2025). Their ubiquity is a direct consequence of continuous discharge from industrial, agricultural, and municipal sources (Fig. 1), coupled with the inadequacy of conventional water and wastewater treatment plants (WWTPs) to effectively remove them (Muambo et al.

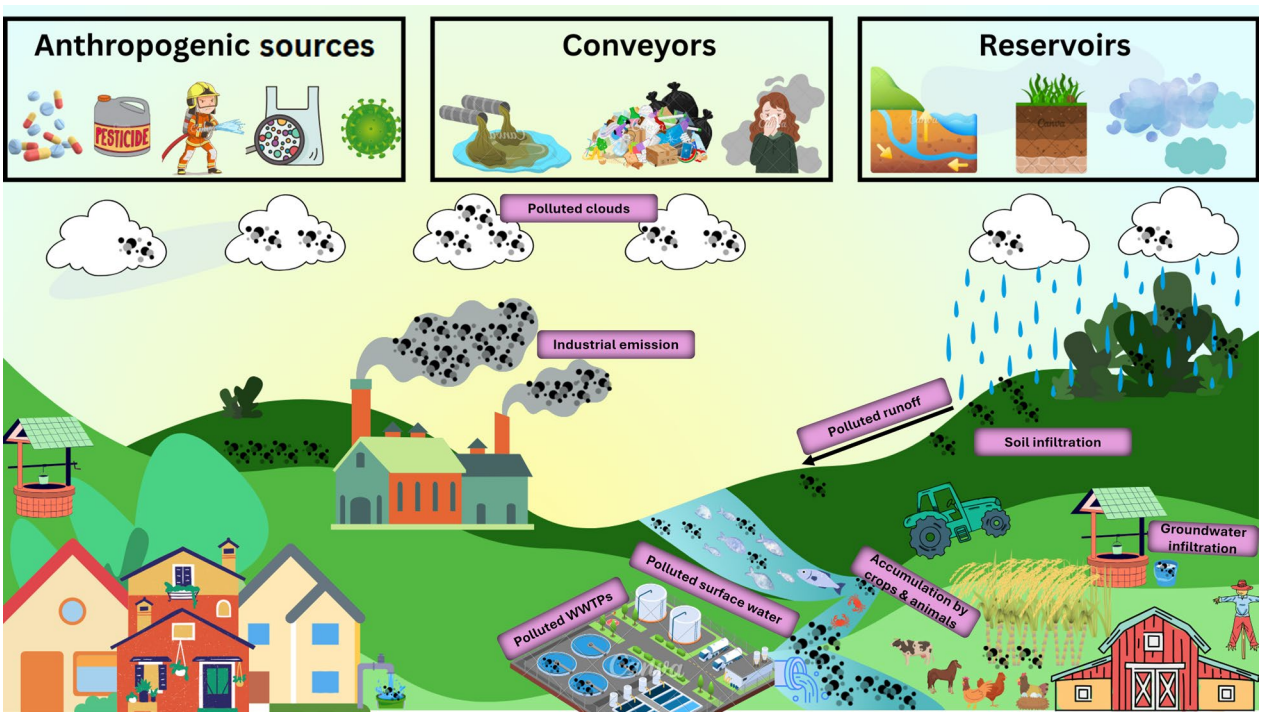


**Fig. 1** Sources, conveyors, and reservoirs of emerging pollutants

2024; Israel et al. 2024). Standard treatment trains often fail to eliminate these recalcitrant compounds, which persist at trace concentrations (ng $L^{-1}$ to μg $L^{-1}$) and can lead to severe long-term consequences such as endocrine disruption, the proliferation of antimicrobial resistance, and bioaccumulation within the food web (Li et al. 2024d; Narain Singh et al. 2025).

EPs have been detected in all hydrological systems, including surface water, groundwater, and potable water resources globally. For example, recent monitoring data from Taihu Lake, China, demonstrated persistent contamination by PFAS congeners, specifically perfluorooctanoic acid (PFOA) and perfluorooctane sulfonate (PFOS), with mean annual concentrations ranging from 21.7 to 25.4 ng $L^{-1}$ and 9.7 to 26.5 ng $L^{-1}$, respectively, over a decade-long surveillance period (Ma et al. 2024a). In a separate investigation of commercially available bottled waters in the Polish market, approximately 35% of the 72 analyzed samples contained quantifiable levels of bisphenol A (BPA), an endocrine-disrupting compound (Wątor et al. 2024). In South America, concentrations of PPCPs have reached up to 270,000 ng $L^{-1}$ in riverine systems (Soriano et al. 2024), while in European surface waters, surfactant levels as high as 45,000 ng $L^{-1}$ have been documented (Assoumani et al. 2024). Beyond chemical contaminants, the biological dimension of EPs is increasingly concerning; antibiotic-resistant organisms and resistance genes (ARGs) have been detected in over 25% of water samples collected from shower hoses and handwash faucets in hospital settings in the Middle East (Gholipour et al. 2024). This global evidence highlights an urgent need to develop advanced, adaptable, and scalable treatment strategies capable of addressing the chemical and biological diversity of EPs. WWTPs must be guided toward tailoring adsorbents and treatment configurations to target their specific contaminant classes.

Adsorption-based technologies have emerged as a highly promising strategy for EP removal due to their operational simplicity and broad applicability. However, the field of adsorbent materials is characterized by a fundamental trade-off, creating a spectrum of solutions with conflicting advantages and disadvantages.

At one end of this spectrum lie high-performance advanced materials. Two-dimensional materials like graphene, with a theoretical specific surface area of 2630 $m^2$ $g^{-1}$, and MXenes ($M_{n+1}X_nT_x$), with their uniquely adaptable surface chemistry, demonstrate exceptional pollutant capture capabilities (Alazmi et al. 2016; Algaradah 2024). Similarly, various engineered nanoparticles (e.g., ZnO, $Fe_3O_4$) and metal–organic frameworks (MOFs) offer superior adsorption capacities and a diverse array of removal mechanisms, including chemisorption, photocatalysis, and antimicrobial action (Hlongwane et al. 2019; Alrefaee et al. 2024).

Despite their technical prowess, their widespread implementation is severely constrained by critical drawbacks. Production costs are often prohibitive; for example, ZnO nanoparticles are estimated at approximately $190,400 USD per ton (Yashni et al. 2021), Cu/Zn bimetallic nanoparticles at $569,000 USD per ton (Noman et al. 2019), and MXenes at a staggering $20.33 million USD per ton (Zaed et al. 2024). Furthermore, their synthesis is frequently energy-intensive, reliant on expensive or hazardous precursors (e.g., hydrofluoric acid for MXene etching), and raises significant environmental and ecotoxicological concerns related to nanoparticle washout and long-term ecosystem impacts (Olawade et al. 2024b).

At the opposite pole is biochar, a carbonaceous material produced from the thermochemical conversion of waste biomass (Liu et al. 2022). Biochar embodies the principles of a circular economy, transforming agricultural residues, forestry waste, and even municipal biosolids into valuable products (Samuel Olugbenga et al. 2024). Its primary advantages are its profound sustainability and low cost, with production estimates around $144 USD/ton (Pandit et al. 2018), making it orders of magnitude cheaper than many advanced nanomaterials. However, the performance of pristine biochar is often moderate. Its removal mechanisms are typically dominated by physisorption (e.g., pore-filling, hydrophobic interactions), which can be non-selective and less effective for highly persistent or polar EPs (Dong et al. 2023).

While numerous reviews have examined the synthesis, modification, and application of biochar for water treatment in isolation, a comprehensive 'design-to-deployment' roadmap that integrates material choice with practical implementation remains lacking. This review addresses the critical gap by proposing a tiered deployment strategy, classifying materials into three tiers: Tier 1 (Pristine Biochar), Tier 2 (Modified Biochar), and Tier 3 (Advanced Biochar Composites). This classification guides selection based on the complexity of the emerging pollutants, treatment objectives, and resource constraints. Beyond performance evaluation, this work uniquely integrates AI-guided engineering, illustrating how predictive modelling can accelerate the development of tailored adsorbents with optimized properties. Furthermore, we provide a holistic scalability assessment that integrates techno-economic analysis (TEA), life-cycle assessment (LCA), and ecotoxicological trade-offs, contextualized through practical case scenarios with defined system boundaries and functional units. Ultimately, this work serves as a one-stop blueprint guiding researchers from foundational principles to the responsible and effective deployment of next-generation biochar technologies.

## 2 Biochar: a tunable foundation for EP removal (Tier 1)

Biochar's effectiveness, both as a standalone adsorbent for EPs and as a foundational platform for advanced composites, is rooted in its inherent and highly tunable physicochemical properties. Feedstock composition and pyrolysis conditions are the critical determinants that allow biochar to be engineered for specific applications. Optimal conversion parameters (such as temperature of 400–700 °C, heating rate of 5–30 °C $min^{-1}$; residence time of 20–120 min, and carrier gas flow rate of 50–150 mL $min^{-1}$ (Leng et al. 2021) and energy-efficient alternative like microwave with power as low as 385 W (Liu et al. 2025c) are crucial for developing desired physicochemical characteristics like specific surface area, pore architecture, and surface functionality (Gwenzi et al. 2017; Mariyam et al. 2025). This inherent tunability directly influences the material's capacity for EP removal through a variety of mechanisms, including electrostatic interactions, π–π electron donor–acceptor (EDA) interactions, hydrogen bonding, hydrophobic partitioning, pore filling, and ion exchange (Fig. 2) (Li et al. 2025b). The efficacy of these mechanisms, particularly pH-sensitive interactions like electrostatic attraction and hydrogen bonding, is also governed by environmental conditions, underscoring the importance of tailored design for specific water matrices (Rajapaksha et al. 2016).

### 2.1 Influence of feedstock and pyrolysis conditions on EP removal

Temperature and heating rate are the most critical parameters governing the final structure and chemistry of biochar (Fan et al. 2021; Li et al. 2024c). Higher pyrolysis temperatures (e.g., > 700 °C) promote greater carbonization and aromatization (Fig. 3), leading to a more graphitic, stable structure with increased surface area and hydrophobicity (Ma et al. 2019). For example, wood biochar produced at a lower temperature resulted in significantly lower surface area—1041.6 $m^2$ $g^{-1}$ at 900 °C versus 3 $m^2$ $g^{-1}$ at 450 °C (Mohan et al. 2012; Machado et al. 2025). High-temperature biochar is ideal for adsorbing non-polar organic pollutants via π–π interactions and hydrophobic partitioning (Choi et al. 2020). Conversely, lower temperatures (e.g., 400–600 °C) preserve a greater number of native oxygen-containing functional groups (–OH, –COOH), which enhance surface hydrophilicity and provide active sites for adsorbing polar pollutants and for subsequent chemical functionalization or nanoparticle anchoring (Clurman et al. 2020). The heating rate influences the residence time of volatile compounds, affecting secondary char formation and final yield.

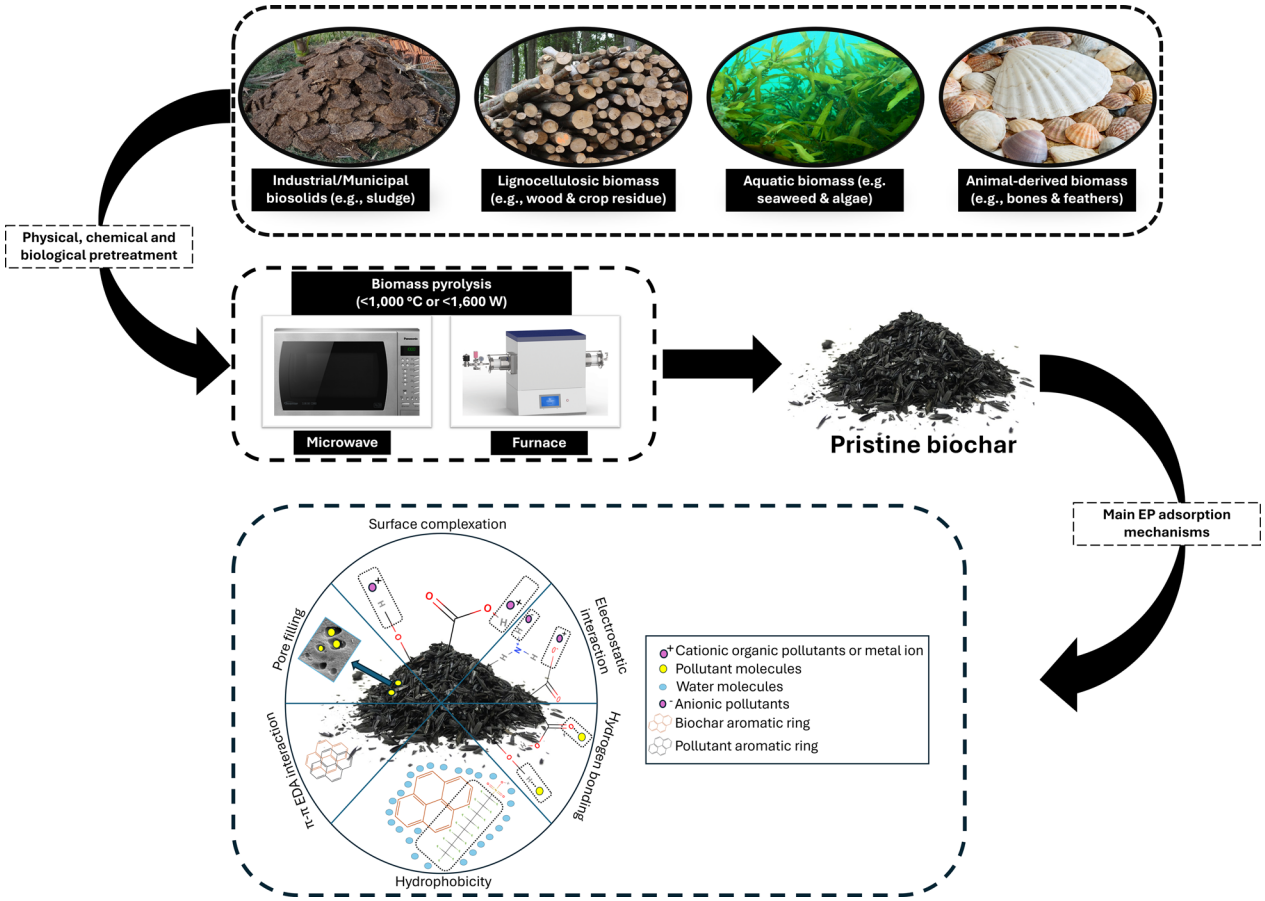


**Fig. 2** Schematic of synthesis of pristine biochar (Tier 1) and an overview of predominant adsorption mechanisms

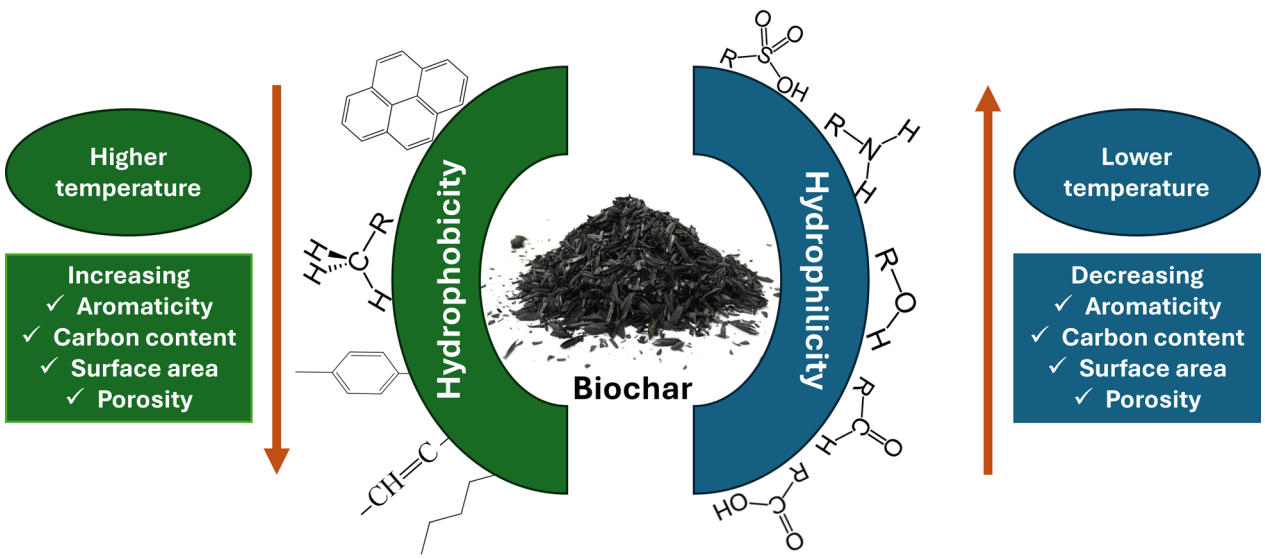


**Fig. 3** Biochar hydrophobic-hydrophilic interactions based on surface functional groups

The choice of raw biomass fundamentally dictates the biochar's inherent characteristics. Lignocellulosic feedstocks (e.g., wood, corn stover, rice husks) are rich in cellulose, hemicellulose, and lignin (Abolore et al. 2024), which upon pyrolysis yield biochars with high carbon content, structural stability, and often well-developed porosity (Gotore et al. 2024). In contrast, feedstocks derived from animal manure, sewage sludge, bone, or microbial biomass are typically richer in proteins and minerals. While these may produce biochars with lower surface areas due to higher ash content (Piccirillo et al. 2017; Achieng et al. 2019), they offer the significant advantage of providing intrinsic heteroatom doping (e.g., nitrogen and sulfur from proteins) and inherent mineral catalysts (e.g., iron, calcium, magnesium from sludge), which can create active sites for specific chemical interactions or catalytic processes (Yin et al. 2020; Yang et al. 2023). For hard carbon production used as an anode material in rechargeable battery systems, feedstocks such as resin-derived carbon and acetylene black are commonly employed (Yang et al. 2025b).

To provide a clearer understanding of these relationships, Table 1 classifies biochars into three main categories based on feedstock origin: (1) wood and cellulose-based, (2) biosolid- or sludge-derived, and (3) bone-based biochars. Generally, wood and cellulose-based biochars exhibit the highest specific surface areas (often exceeding 1000 $m^2\ g^{-1}$ at elevated pyrolysis temperatures of ≥ 900 °C) as the volatilization of lignocellulosic components enhances pore development (Machado et al. 2025). In contrast, sludge biochars tend to display lower surface areas (typically < 100 $m^2\ g^{-1}$) due to their higher ash and mineral contents, although their inherent heteroatoms and metal oxides can promote catalytic adsorption even when surface area is limited (Regkouzas and Diamadopoulos 2019). Bone-based biochars, produced from calcium- and phosphate-rich matrices, require higher pyrolysis temperatures (≥ 700–1000 °C) to achieve comparable porosity owing to their dense inorganic structure (Piccirillo et al. 2017).

Despite these differences, Table 1 demonstrates that surface area is not the sole determinant of adsorption efficiency, some low-surface-area biochars still achieve notable EP removal through chemical bonding, complexation, or ion-exchange mechanisms, highlighting the diverse functional potential of pristine biochar systems (Mohan et al. 2012).

### 2.2 Modified biochar for enhanced remediation of EP in water (Tier 2)

Beyond initial synthesis, a suite of modification techniques can be employed to further engineer the biochar platform for specific applications. These strategies can be broadly categorized by their impact on surface/pore structure and surface chemistry. As highlighted in Fig. 4, activation methods are designed to dramatically increase the surface area and tailor the pore size distribution (Hu et al. 2020), while surface chemistry engineering methods modify the electronic properties and functionality of the biochar surface (Li et al. 2025b).

Chemical activation involves impregnating the biomass or biochar with chemical agents like $H_3PO_4$ or KOH prior to or during thermal treatment. $H_3PO_4$ acts as a dehydrating agent and template, creating a highly porous structure with enhanced microporosity and leaving behind phosphate functional groups that can aid in metal binding (Chu et al. 2018). KOH activation at high temperatures creates a molten salt that etches the carbon framework, generating ultra-high surface areas, with values reported to exceed 3300 $m^2\ g^{-1}$, and a predominantly microporous structure ideal for trapping small pollutant molecules (Dou et al. 2022). $ZnCl_2$ is also a highly effective activating agent; its thermal decomposition promotes extensive pore formation, increasing the surface area of corn cob biochar from ~ 6 to 1201 $m^2\ g^{-1}$ at 700 °C (Varela et al. 2024).

Physical activation offers a chemical-free alternative. Steam activation uses water vapor at high temperatures to gasify a portion of the carbon, creating and widening pores (Shi et al. 2022a). Ball milling is a mechanical method that can increase surface area by fracturing particles and can also introduce oxygen-containing functional groups through reactions with atmospheric oxygen at the newly created surfaces (Lyu et al. 2018; Zhuang et al. 2021).

Heteroatom doping intentionally introduces non-carbon elements (e.g., N, S, P, and B) into the carbon lattice (Chen et al. 2023; Li et al. 2024b). Nitrogen doping is particularly effective, as nitrogen's electronegativity creates charge differentials and structural defects that act as active sites for both adsorption (via enhanced π–π electron donor–acceptor interactions and hydrogen bonding) and catalytic reactions (Guo et al. 2016; Li et al. 2025b).

Co-pyrolysis represents a highly versatile route for simultaneous activation and heteroatom doping of biochar through the thermal co-conversion of two or more feedstocks. The synergistic interactions among precursors enable in-situ modification of the carbon matrix without the need for external activation agents. For instance, lignocellulosic biomass provides aromatic carbon frameworks, while nitrogen- or metal-rich feedstocks (e.g., algae, sewage sludge, or metal salts) supply dopant elements such as N, S, Fe, or Mn during pyrolysis, producing biochars with tailored surface functionalities and catalytic sites (Liu et al. 2021; Qin et al. 2023). This intrinsic co-doping improves electron

**Table 1** Differences in surface properties and pollutant adsorption capacities of pristine biochar classified by feedstock origin and pyrolysis temperature

| Feedstock | Temperature | Specific surface area | pore volume | pH | Pollutant and adsorption capacity | References |
|---|---|---|---|---|---|---|
| *Wood and cellulose-based biomass* | | | | | | |
| Eucalyptus | 500 °C | 335 $m^2 g^{-1}$ | 0.17 $cm^3 g^{-1}$ | 7 | Fluoxetine—6.41 mg $g^{-1}$ | Fernandes et al. (2019) |
| Eucalyptus tree | 900 °C | 1041.6 $m^2 g^{-1}$ | 0.56 $cm^3 g^{-1}$ | 4 | Naphthenic acid—35 mg $g^{-1}$ | Machado et al. (2025) |
| Bamboo biochar | 500 °C | 665.3 $m^2 g^{-1}$ | 0.24 $cm^3 g^{-1}$ | 3–10 | Fluoroquinolone Antibiotics—45.9 mg $g^{-1}$ | Wang et al. (2015) |
| Dougas fir wood | 900–1000 °C | 700 $m^2 g^{-1}$ | 0.26 $cm^3 g^{-1}$ | 7 | PFOS (14.6 mg $g^{-1}$ and 215 mg $g^{-1}$) and PFOA (9 mg $g^{-1}$ and 53 mg $g^{-1}$) for batch and column capacities | Rodrigo et al. (2022) |
| Wood chips | 750 °C | 900 $m^2 g^{-1}$ | 0.35 $cm^3 g^{-1}$ | ≥7 | PFOA—69.2 mg $g^{-1}$ (at $C_e$ 100 µg $L^{-1}$) | Skjennum et al. (2024) |
| Pine wood/bark | 400 and 450 °C | 1–3 $m^2 g^{-1}$ | – | 2 | Comparable fluoride removal to activated carbon with SA of 1,000 $m^2 g^{-1}$ | Mohan et al. (2012) |
| Corn corb | 600 °C | 306 $m^2 g^{-1}$ | – | 7 | Ciprofloxacin (0.3996 mg $g^{-1}$), Ofloxacin (0.3 mg $g^{-1}$), and Delafloxacin (0.09 mg $g^{-1}$) | Dang et al. (2022) |
| Banana pseudo-stem | 500 °C | 390 $m^2 g^{-1}$ | 0.20 $cm^3 g^{-1}$ | 6–7 | Ofloxacin—0.3–218.3 mg $g^{-1}$ | Wang et al. (2024) |
| Chili seeds | 600 °C | 0.2 $m^2 g^{-1}$ | 0.00017 $cm^3 g^{-1}$ | 7 | Ibuprofen—26.1 mg $g^{-1}$ | Ocampo-Perez et al. (2019) |
| *Biosolid and sludge-derived biomass* | | | | | | |
| Sewage sludge | 300 °C | 13.5 $m^2 g^{-1}$ | – | 7 | BPA—85.4 mg $g^{-1}$ | Regkouzas and Diamadopoulos (2019) |
| Sewage sludge | 500 °C | 53.1 $m^2 g^{-1}$ | 0.082 $cm^3 g^{-1}$ | 7 | Imidacloprid—3.0 mg $g^{-1}$ | Ma et al. (2021) |
| Sludge-derived biochar | 550 °C | 23.5–297.5 $m^2 g^{-1}$ | 0.068–0.16 $cm^3 g^{-1}$ | 7 | Fluoroquinolone antibiotics—4.4–19.8 mg $g^{-1}$ | Yao et al. (2013) |
| Sludge | 600 °C | 39.2 $m^2 g^{-1}$ | 0.15 $cm^3 g^{-1}$ | — | Sulfamethoxazole—0.7 mg $g^{-1}$ | Ma et al. (2024b) |
| Sewage sludge | 600 °C | 283.5 $m^2 g^{-1}$ | – | 7 | BPA—75% removal from 10 µg $L^{-1}$ solution | Birer et al. (2021) |
| Yak Dung | 700 °C | 198.8 $m^2 g^{-1}$ | – | 3–10 | Tetracycline (32.0 mg $g^{-1}$) and Oxytetracycline (26.1 mg $g^{-1}$) | Wu et al. (2019) |
| Sewage sludge | 800°C | 375 $m^2 g^{-1}$ | 0.14 $cm^3 g^{-1}$ | ≥7 | PFOA: 251.9 mg $g^{-1}$ | Skjennum et al. (2024) |
| *Bone-based biomass* | | | | | | |
| Tilapia fish bone | 550 °C | 124 $m^2 g^{-1}$ | 0.21 $cm^3 g^{-1}$ | | Tetracycline—70 mg $g^{-1}$ | Módenes et al. (2021) |
| Fish scale biochar | 600 °C | 94.1 $m^2 g^{-1}$ | 0.23 $cm^3 g^{-1}$ | 2 | Indigo carmine—10.9 mg $g^{-1}$ | Achieng et al. (2019) |
| Bone | 700 °C | 74 $m^2 g^{-1}$ | 0.093 $cm^3 g^{-1}$ | 7 | Naproxen: 3.2 mg $g^{-1}$ | Reynel-Avila et al. (2015) |
| Tuna bone biochar | 1000 °C | 100.7 $m^2 g^{-1}$ | 0.58 $cm^3 g^{-1}$ | – | Tramadol—2.1 mg $g^{-1}$ and Venlafaxine—1.7 mg $g^{-1}$ | Miranda et al. (2024) |
| Fish bone biochar | 1000 °C | 80.0 $m^2 g^{-1}$ | – | <6 | Diclofenac (43.3 mg $g^{-1}$) and Fluoxetine (55.9 mg $g^{-1}$) | Piccirillo et al. (2017) |

transfer, enhances oxidant activation [e.g., peroxymonosulfate (PMS)], and mitigates metal leaching often associated with single-metal modifications (Diao et al. 2023; Wang et al. 2023). Moreover, alkali and alkaline earth metals released during co-pyrolysis promote self-activation by catalyzing dehydrogenation and

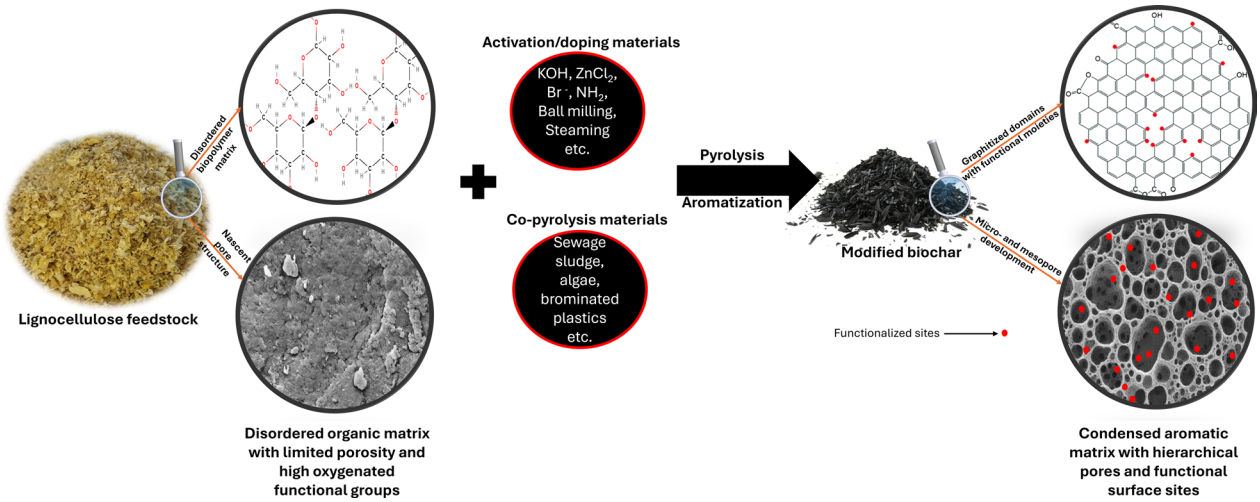


**Fig. 4** Schematic of Tier 2 (Engineered Biochar) production via in-situ modification. This single-step process simultaneously transforms the amorphous polymeric structure into a highly porous, aromatic carbon structure while embedding active functionalized sites (red dots)

micropore formation, significantly improving surface area and porosity (Sevilla et al. 2021; Cheng et al. 2022). Notably, studies have demonstrated that co-pyrolysis can achieve adsorption capacities up to 844 mg $g^{-1}$ for sulfamethoxazole via potassium- and iron-driven self-activation (Qin et al. 2023). Co-pyrolysis of wood waste and plastic waste was also reported to yield Br-functionalized biochar, which efficiently adsorbed $Hg^0$ (Xu et al. 2018). Therefore, co-pyrolysis serves as an energy-efficient, one-step process that integrates structural activation, chemical doping, and catalytic enhancement, offering a sustainable pathway for designing multifunctional biochars optimized for emerging pollutant remediation.

The application of these engineering strategies consistently results in biochars with superior performance for EP removal in water. As detailed in Table 2, modifications such as heteroatom doping and activation can enhance adsorption capacities by orders of magnitude for a wide range of EPs, including pharmaceuticals, heavy metals, and organic pollutants, when compared to their pristine counterparts in Table 1. Among these methods, chemical activation appears most promising for achieving dramatic improvements, with KOH activation yielding biochar with an ultra-high surface area of up to 3370 $m^2$ $g^{-1}$ and an extraordinary adsorption capacity of over 1000 mg $g^{-1}$ for ciprofloxacin (Dou et al. 2022). In other instances, potassium ferrate ($K_2FeO_4$) has been used for dual modification as it decomposes in solution to form iron oxide and KOH (Zhang et al. 2025). Chemical activation processes via co-pyrolysis have been reported to be improved by adding molten salts like $ZnCl_2$/KCl as a reaction medium, reducing reaction time and temperature and enhancing mass transfer (Liu et al. 2025c).

## 3 Advanced biochar composites for targeted EP removal (Tier 3)

While biochar has garnered significant attention as a sustainable adsorbent for various pollutants, its effectiveness against EPs can be limited, particularly at higher concentrations or in complex mixtures. Although biochar offers advantages such as low cost, widespread availability, and alignment with circular economy principles, its performance in EP removal is often constrained by a reliance on predominantly physisorption mechanisms, limited selectivity, and potential particle aggregation at higher dosages, which reduces the specific surface area and accessible binding sites (Dong et al. 2023). Conversely, advanced materials, including engineered nanomaterials (ENMs), graphene, and 2D materials like MXenes, exhibit superior adsorption capacities and offer a wider array of removal mechanisms, such as chemisorption, photocatalytic degradation, and specific molecular interactions (Rikta 2019; Olawade et al. 2024a, b; Alyasi et al. 2024). However, these materials often face challenges related to high production costs, potential environmental impacts, and difficulties in recovery and reuse.

A promising approach to overcoming these limitations lies in the development of biochar-based composites, which synergistically integrate biochar's sustainability and cost-effectiveness with the enhanced functionalities of advanced materials. These composites can be synthesized through various strategies broadly categorized into pre-treatment and post-treatment methods. Pre-treatment (in-situ) methods involve modifying the raw

**Table 2** Forms of biochar engineering to improve surface and adsorption properties

| Material | Process | Surface area ($m^2 g^{-1}$) | Volume ($cm^3 g^{-1}$) | Adsorption capacity | References |
|---|---|---|---|---|---|
| *Heteroatom doping* | | | | | |
| Maize straw | N/B doping | 254.74–713.52 | 75–350 | Sulfamethoxazole—32.4–90.4% | Sui et al. (2025) |
| Poplar powder | N/S doping | 12.23–336.8 | 0.052–0.186 | BPA—0.8–4.5 mg $g^{-1}$ | Yu et al. (2025) |
| Waste wood and computer casing plastic | Fe/Br doping | 3.29–71.06 | < DL to 0.0057 | Mercury—0.353–0.914 mg $g^{-1}$ | Sun et al. (2025b) |
| Pig bone | N doping | 1613–1287 | 2.4 folds higher | Tetracycline—396.4–481.6 mg $g^{-1}$ | Xia et al. (2025) |
| Hydroxymethylcellulose | P doping | 956.97–1307.30 | 0.62–0.94 | Tetracycline—119.81–155.55 mg $g^{-1}$ | Fu et al. (2024) |
| *Co-pyrolysis* | | | | | |
| Plastic computer shell and wood | Br doping | 39.45–11.26 | 9.06–2.87 | $Hg^0$—50–90% | Xu et al. (2018) |
| Spirulina with $FeCl_3$ | Fe doping | 98.43–395.76 | 0.10–0.22 | Sulfathiazole—40.04–106.62 mg $g^{-1}$ | Diao et al. (2023) |
| Peanut shell, urea, and sulfur powder | N/S doping | 706–863 | 0.30–0.38 | Phenol—20–99% | Li et al. (2023a) |
| *Chemical activation* | | | | | |
| Fish scale | KOH activation | Up to 3370 | Up to 1.91 | Ciprofloxacin—> 1000 mg $g^{-1}$ | Dou et al. (2022) |
| Bamboo dust | Phytic acid activation | 12–1298 | 0.015–0.919 | U(VI)—10–140 mg $g^{-1}$ | Hu et al. (2020) |
| Pine sawdust | $H_3PO_4$ | ~ 400 to ~ 1600 | ~ 0.2 to ~ 0.9 | BPA and carbamazepine—< 30 to ~ 220 mg $g^{-1}$ | Chu et al. (2018) |
| Water hyacinth | KOH | 38.57–2412.58 | – | Tetracycline—34.25 and 28.94 mg $g^{-1}$ and Cr (VI)—83.89 and 115.28 mg $g^{-1}$ | Qu et al. (2021) |
| *Physical activation* | | | | | |
| Pine wood sawdust | Ball milling | 230.43–354.62 | – | Acetone ~ 175 to ~ 300 mg $g^{-1}$ Toluene ~ 30 to ~ 150 mg $g^{-1}$ | Zhuang et al. (2021) |
| Tea waste | Steaming | 342.2–576.1 | 0.022–0.109 | Sulfamethazine—0.04–1.57 mg $g^{-1}$ $min^{-1}$ | Rajapaksha et al. (2016) |
| Douglas fir biochar | Magnetization with $Fe_3O_4$ | 468.2–322.0 | 0.193–0.120 | Adsorption increased from 24.6 to 75.1 mg $g^{-1}$ for caffeine, 17.5 to 39.9 mg $g^{-1}$ for ibuprofen and 106.2 to 149.9 mg $g^{-1}$ for acetylsalicylic acid | Liyanage et al. (2020) |

biomass before or during pyrolysis, such as by impregnating the feedstock with metal salts or by co-pyrolyzing the biomass with functional additives like metal oxides (Pan et al. 2021). In contrast, post-treatment (ex-situ) methods such as impregnation, co-precipitation, and evaporation-assisted deposition load nanoparticles or 2D materials onto the surface of preformed biochar, offering higher control over loading efficiency and surface functionalization (Yang et al. 2025a, b). Other promising methods include ball milling, which achieves mechanical integration without hazardous reagents. For detailed mechanistic and process-specific discussions, readers are referred to comprehensive reviews by Pan et al. (2021) and Yang et al. (2025a, b).

Beyond improving adsorption efficiency, these hybrid materials introduce additional removal mechanisms, including photocatalysis, electrocatalysis, antimicrobial action, molecular sieving, Fenton reactions, and catalytic ozonation (Fig. 5). For instance, MXene composites have demonstrated molecular sieving capabilities,

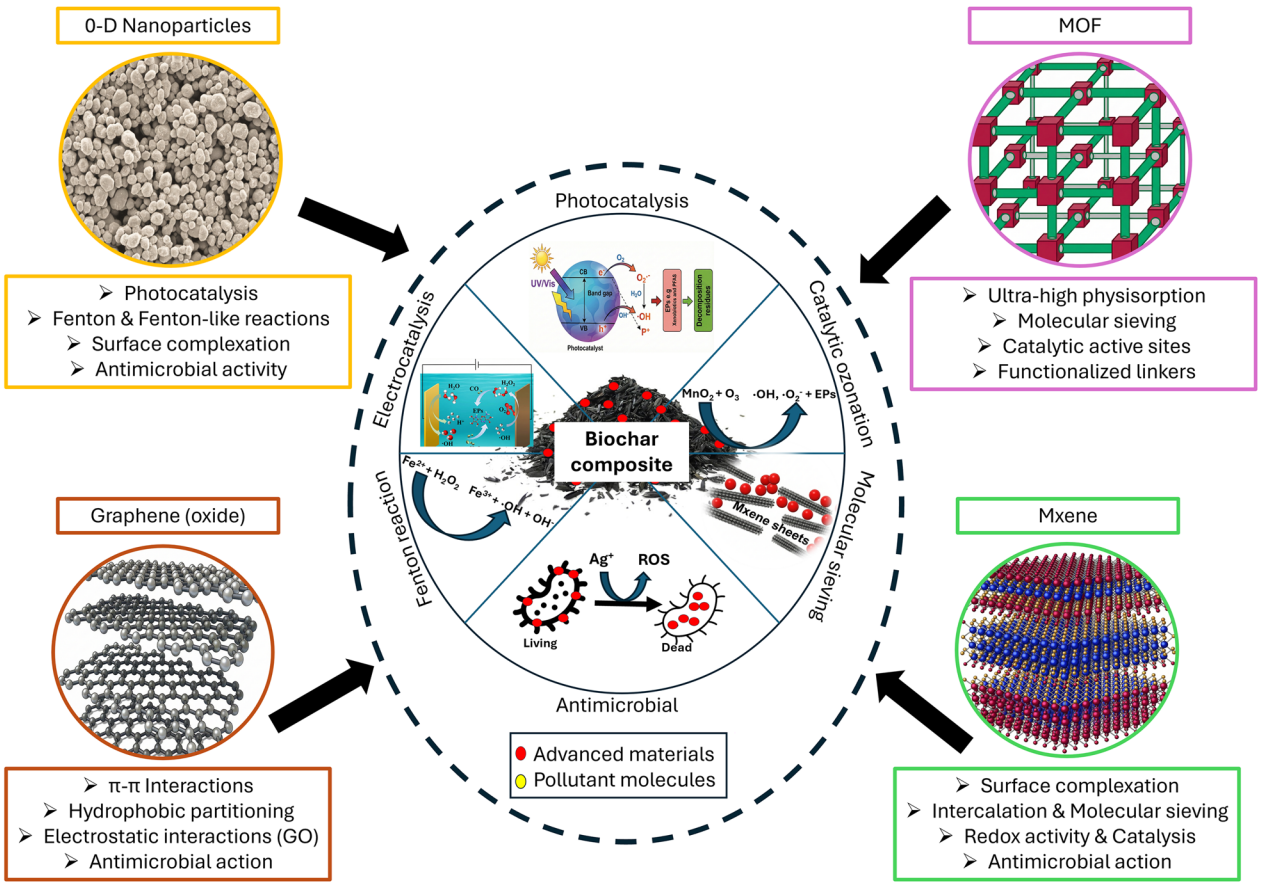


**Fig. 5** A breakdown of the enhanced removal mechanisms contributed by key classes of advanced materials. This figure illustrates how incorporating Graphene/GO, MXenes, Nanoparticles (NPs), and Metal–Organic Frameworks (MOFs) into biochar composites provides a suite of advanced functionalities

as exemplified by Yang et al. (2024), who engineered MXene-cellulose nanofiber membranes with exceptional selectivity and permeability. Their optimized MXC-3-L membrane achieved > 99% rejection of Congo red and effectively removed PFAS with a nearly eightfold increase in permeance compared to commercial polyamide membranes. Similarly, biochar-nanoparticle hybrids have shown promise in Fenton-based degradation, catalytic ozonation, and electrocatalysis, significantly enhancing the breakdown of persistent organic pollutants (Ahmaruzzaman 2021; Nidheesh et al. 2024; Li et al. 2025a). This section explores how these synergistic interactions expand the removal pathways for EPs, with specific examples of composites targeting key EPs, such as PFAS, microplastics, pharmaceuticals, endocrine disruptors, pesticides, emerging pathogens, and emerging inorganic metals. The section ends by summarizing pollutant-specific design principles mapped across the three biochar tiers, highlighting how structural, chemical, and functional attributes can be tuned to maximize removal efficiency for diverse emerging pollutant classes (Table 3).

### 3.1 PFAS

Although biochar offers promise as a sorbent for PFAS, its adsorption capacity and removal efficiency can be significantly improved through strategic composite modifications. A prominent approach involves the incorporation of cationic polymers, most notably polyethyleneimine (PEI), onto either the biochar surface or functionalized nanoparticles. This modification introduces a high density of positively charged amine functional groups ($–NH_2^+$). These amine groups facilitate strong electrostatic interactions with the negatively charged sulfonate ($–SO_3^-$) or carboxylate ($–COO^-$) head groups of PFAS molecules, leading to significantly enhanced adsorption (Smaili and Ng 2023). For instance, Lee et al. (2023) reported ultra-high sorption capacities for PFOA (18.3 mmol $g^{-1}$) and PFOS (88.8 mmol $g^{-1}$) using PEI-coated superparamagnetic iron oxide nanocrystals (IONCs), substantially surpassing the performance of traditional activated carbon. The creation of biochar-magnetic nanoparticle composites, especially those functionalized with cationic polymers

**Table 3** Tiered remediation strategies for key emerging pollutants

| Pollutant type | Tier 1: Pristine Biochar | Tier 2: Modified Biochar | Tier 3: Advanced composites | References |
|---|---|---|---|---|
| PFAS (e.g., PFOA, PFOS) | Biochar (BC) with high aromaticity (≥ 600 °C), high porosity (pore size > 1.5 nm); positively charged surface (pHpzc > operating pH) to favour electrostatic attraction | Surface cationic functionalization (e.g., PEI, chitosan); enhanced hydrophobic domains | Magnetic and fluorous composites (e.g., $Fe_3O_4$/BC, MXene/BC) enabling electrostatic + fluorous interactions + redox removal; reusable via magnetic separation | USEPA (2017), Lin et al. (2022), Krebsbach et al. (2023), Lee et al. (2023), Musegades et al. (2024), He et al. (2024), Wang et al. (2025a) |
| Pharmaceuticals (e.g., Carbamazepine) | Aromatic biochar (from lignocellulosic sources); microporous dominant with high surface area; oxygenated groups | Chemical activation (e.g., KOH) to create ultra-high microporosity and N/S doping to enhance π–π EDA interactions and H-bonding | $TiO_2$-BC or CuO-BC enabling photocatalytic degradation + adsorption synergy; GO/BC for enhanced π–π and H bonding | Chen et al. (2017a, b), Li et al. (2019), Liang et al. (2020), Zhang et al. (2023) |
| Endocrine Disruptors (e.g., Bisphenol A) | Hierarchical micro/mesoporous BC; surface charge tuning (pHpzc > pH); aromatic domains | Fe/N co-doped BC for active site enrichment; template methods for hierarchical porosity | Graphene-BC composites for π–π and hydrophobic partitioning + Fe/N/Mn co-doping for AOP activity | Heo et al. (2019), Vasiljevic and Harner (2021), Shi et al. (2022b), Ding et al. (2022), Zhou et al. (2023), Abu Hasan et al. (2023) |
| Pesticides (e.g., Atrazine) | Polar BC (high O/C & N/C ratio); low pyrolysis temperature (< 500 °C); high CEC | Fe doped BC to enhance redox and AOP activity | g-$C_3N_4$-BC or $TiO_2$-BC photocatalytic hybrids for mineralization and adsorption | Song et al. (2024), Afzal et al. (2025), Peng et al. (2025) |
| Emerging pathogens/ARGs | Biochar with well-developed mesopore and macropores; positively charged surface | Cationic functionalization (e.g., amination); Fe/N co-doped BC enhancing electron transfer and antimicrobial activity | UiO-66-MXene–BC, BiOCl-NP, and AgNP–BC composites for antibacterial and DNA degradation capacity and photocatalytic degradation | Khatami et al. (2022), Mishra et al. (2024), Sun et al. (2025a), Gholap et al. (2025), Min et al. (2025) |
| Inorganic Oxyanions (e.g., Cr(VI), As(V)) | Lower-temp biochar (< 500 °C) with protonated functional groups; high CEC | Metal oxide-loaded BC (e.g., Fe, Mn, ZnO) for redox reduction and surface complexation | MOF–BC composites combining chelation, ion exchange, and catalytic redox transformation | Dzoujo et al. (2024), Ghaedi et al. (2025), Shaheen et al. (2025) |
| Microplastics and nanoplastics | Microporous biochar (> 700 °C for nano) for physical entrapment and hydrophobic interactions | Magnetic ($Fe_3O_4$) and metal modified (Mg/Zn) biochar for increased surface roughness, complexation of functionalized plastics and separation | Composites with magnetic carbon nanotubes or Chitin-graphene oxide sponges for enhanced electrostatic, hydrogen bond, and π–π interactions | Sun et al. (2020), Tang et al. (2021), Singh et al. (2021a), Ganie et al. (2021), Wang et al. (2021) |

like PEI, offers a dual advantage: high PFAS adsorption capacity and facile magnetic separation, enabling efficient sorbent recovery and reuse. Li et al (2022) further demonstrated this principle using a plant-derived biomimetic nano-framework modified with PEI, achieving remarkable PFOA and PFOS adsorption capacities ranging from 3529 to 4151 mg $g^{-1}$. This highlights the potential of biochar as a foundational component in advanced, multifunctional composite materials. Further demonstrating the importance of electrostatic interactions and amine functionalization, Lu et al. (2024) achieved 95.4% removal of sodium p-per fluorous nonenoxybenzene sulfonate, a PFAS alternative within 120 min using chitosan-modified amino-driven GO composite. Beyond electrostatic interactions, the concept of "fluorous interactions" presents another promising avenue for enhancing PFAS removal. As explored by Tan et al. (2021) and He et al. (2024), the strong affinity between fluorinated sorbent components, such as amphiphilic perfluoropolyether (PFPE)-containing block copolymers, and the perfluorinated alkyl tails of PFAS molecules can significantly improve selectivity and mitigate the competitive effects of co-contaminants. This approach has demonstrated PFOA removal efficiencies exceeding 90%, even in complex matrices like fetal bovine serum. Pore size matching pollutant dimensions is also crucial, as seen in PFOA removal where sludge biochar's mesopores (3–6 nm) were more effective than wood-derived biochar's smaller pores of 1.5 nm (Skjennum et al. 2024).

For specific pollutants like PFAS, which maintain negative charges across the pH spectrum due to low pKa values (−3.27 for PFOS, −0.2 for PFOA) (Zhang et al. 2019), hydrophobic interactions often dominate over electrostatic forces. The strong hydrophobicity of the C–F region, contrasting with the hydrophilic –COOH and $–SO_3H$ terminal groups, enables adsorption through hydrophobic interactions that can overcome electrostatic repulsion (Guo et al. 2017; Hassan et al. 2020; Behnami et al. 2024). This mechanism is particularly effective for long-chain PFAS compounds, while short-chain variants require enhanced hydrophobicity of the adsorbent material (Zaggia et al. 2016).

### 3.2 Pharmaceuticals

Although, conventional adsorbents like biochar and activated carbon can remove PhACs from water, their effectiveness is often limited, especially in complex mixtures where multiple pharmaceuticals compete for available adsorption sites (Całus-Makowska et al. 2024). For example, the addition of copper oxide (CuO) to biochar has also been shown to enhance the chemical adsorption of some pharmaceuticals, such as ciprofloxacin, diclofenac, and carbamazepine (CBZ), indicating a role for metal oxides in tuning biochar surface properties via increased active sites for improved pollutant removal (Liang et al. 2020; Xue et al. 2022). Besides enhanced adsorption in complex systems, biochar composites also facilitate subsequent regeneration and reuse. For instance, Wurzer et al. (2019) demonstrated that Fe-biochar composites exhibited improved degradation of a mixture of ten pharmaceuticals (including antibiotics, fungicides, and antidepressants) during hydrothermal treatment. This resulted in lower required treatment temperatures for complete decontamination compared to pristine biochars, highlighting the potential for enhanced regenerability and reduced energy consumption (Wurzer et al. 2019, 2020). Engineered biochar composites also offer a promising avenue for enhancing the removal of recalcitrant PhACs, including CBZ (Zhang et al. 2023). Combining biochar with materials like GO significantly improves adsorption capacity due to increased π–π interactions between the aromatic rings of CBZ and the graphene-like surface. Agilandeswari et al. (2024) demonstrated that a polypyrrole-graphene oxide-biochar (Ppy-GO-Biochar) composite achieved a maximum CBZ sorption capacity of 45.04 mg $g^{-1}$, outperforming many other adsorbents, including standard activated carbon and pristine biochars, and showcasing the significance of the biochar-GO synergy. Although carbon nanotubes and graphene oxide individually exhibit high adsorption capacities for CBZ (up to 7910 mg $g^{-1}$ and 215 mg $g^{-1}$, respectively) (Oleszczuk et al. 2009; Cai and Larese-Casanova 2014), their high-cost limits large-scale application (Chen et al. 2017a). Integrating a smaller, more sustainable fraction of these materials into a biochar matrix capitalizes on their superior adsorption properties while maintaining cost-effectiveness. Further, beyond adsorption, incorporating components that promote photocatalytic degradation offers a synergistic approach. Li et al. (2019) developed a magnetically separable $Fe_3O_4$/BiOBr/biochar composite that achieved 95.51% CBZ photodegradation under visible light irradiation, highlighting the potential of combining adsorption with AOPs.

Environmental pH could influence the effectiveness of remediation. The complexity of pH-dependent adsorption is highlighted by studies on sulfamethoxazole (SMX), where mechanisms shift from pore filling and $\pi^+$–π EDA interactions in acidic conditions to pore filling and negatively charge-assisted hydrogen bonding (CAHB) in alkaline conditions (Li et al. 2023c). Similar pH-dependent interplay was seen with sulfapyridine adsorption on cotton gin waste biochar, while other pharmaceuticals showed pH-independent behaviour (Ndoun et al. 2021).

### 3.3 Microplastic

Microplastics and nanoplastics have recently been considered for removal using biochar-composites. Pristine biochar, particularly when produced at high pyrolysis temperatures (750 °C), has demonstrated exceptional nanoplastic removal (> 99%) with rapid equilibrium (< 5 min) and an adsorption capacity of 44.9 mg $g^{-1}$ (Ganie et al. 2021). Its effectiveness extends to real-world scenarios, with pinewood and sugarcane biochars achieving 86.6–92.6% removal of various microplastics from farm runoff (Olubusoye et al. 2024). The removal mechanisms are largely physical and chemical, including physical entrapment, hydrophobic behaviour, and electrostatic interactions, with microscopic analysis revealing that microplastics are effectively immobilized by being 'stuck', 'trapped', and 'entangled' within the biochar's porous, honeycomb-like structures, achieving over 95% removal of 10 µm spheres (Wang et al. 2020; Olubusoye et al. 2024). Interestingly, studies on biochars with relatively low surface areas (200–600 $m^2$ $g^{-1}$) show they are highly suitable for microplastics removal, suggesting that ultra-high porosity is not always necessary for effective water purification and supporting the economic feasibility of bio-based adsorbents (Siipola et al. 2020).

The efficacy can be significantly enhanced by creating composites. For instance, magnetic biochar ($Fe_3O_4$-biochar) more effectively inhibits plastic particle transport than pristine biochar due to increased surface roughness and favourable surface charge alterations (Tong et al. 2020). Iron-modified magnetic biochars pyrolyzed at 850 °C have achieved rapid removal (< 10 min) and high maximum capacities of 225.11 mg $g^{-1}$ for carboxylated nanoplastics, primarily through surface complexation mechanisms (Singh et al. 2021a). Similarly, Mg/Zn-modified magnetic biochars reached removal efficiencies of up to 99.46% for 1 µm polystyrene spheres and demonstrated excellent reusability, maintaining > 95% efficiency after five adsorption-pyrolysis cycles where the metals catalyzed microplastic degradation during thermal regeneration (Wang et al. 2021). Materials not yet combined with biochar, such as magnetic carbon nanotubes (M-CNTs) with an extraordinary removal capacity of up to 1650 mg $g^{-1}$ for polyethylene (Tang et al. 2021), and chitin-graphene oxide (ChGO) sponges that utilize electrostatic, hydrogen bond, and π–π interactions (Sun et al. 2020), could be suitable candidates for creating next-generation biochar composites. However, it is crucial to consider that the sorption efficiency of these materials can be negatively impacted by environmental factors like alkaline pH, humic acid, and competing ions in real water matrices (Ganie et al. 2021; Wang et al. 2021).

### 3.4 Bisphenol A

While pristine biochar exhibits limited BPA adsorption capacity, strategic modifications can drastically improve its performance. Research highlights the remarkable effectiveness of multi-element doping, particularly the co-doping of biochar with Fe, Mn, Cu, and Ding et al. (2022) demonstrated that Fe–Mn–N co-doped biochar achieved a BPA adsorption capacity of 48.64 mg $g^{-1}$, more than 11 times higher than that of the undoped biochar. This enhancement is attributed to the creation of active sites (Fe-$N_x$ and graphitic N) and modifications to the biochar's electron cloud density, promoting stronger interactions with BPA. Another key strategy is to engineer biochar with a hierarchically porous structure and high surface area. Shi et al. (2022b) utilized a template method with colloidal silica and $ZnCl_2$ activation to produce hierarchically porous biochar with an exceptionally high surface area (up to 2944 $m^2$ $g^{-1}$) and a BPA adsorption capacity reaching 908.8 mg $g^{-1}$ at higher BPA concentrations, showcasing the importance of maximizing accessible adsorption sites. Crucially, this hierarchical porosity includes a significant proportion of mesopores, which facilitate the transport of BPA molecules to the internal adsorption sites within the micropores and enhance overall adsorption kinetics (Shi et al. 2022b). It is worth noting that optimizing the synthesis to maximize the hierarchical porosity is essential for BPA adsorption. In another study by Heo et al. (2019), a biochar-supported magnetic $CuZnFe_2O_4$ composite was reported to have significantly higher BPA adsorption capacity (263.2 mg $g^{-1}$) than pristine (185.2 mg $g^{-1}$) due to the presence of the more pores and active sites to aid BPA interactions. The synergistic effect of the different modifications has been found to be very effective and shows that the combination of the optimal characteristics discussed earlier can improve the performance of biochar. Solution pH also plays a role, with adsorption generally favoured under neutral to slightly acidic conditions where BPA is predominantly in its molecular form (Heo et al. 2019).

### 3.5 Atrazine

Although adsorption of atrazine onto standard biochar has been reported to be effective (Tan et al. 2016; Hernandes et al. 2022), advanced composite modifications offer substantial improvements in atrazine removal, often combining adsorption with degradation pathways. A prominent strategy is to integrate biochar with photocatalytic materials. Peng et al. (2025) demonstrated a 4.9-fold improvement in atrazine photocatalytic degradation using nitrogen vacancy-mediated carbon nitride

modified with deep eutectic solvents, highlighting the potential of metal-free photocatalysts. Similarly, Altendji and Hamoudi (2024) showed that a g-$C_3N_4$/$TiO_2$/$NiFe_2O_4$ composite, especially when combined with PMS, achieved 97.2% atrazine conversion. Perovskite materials, particularly nano-cast $LaCoO_3$, also exhibit high catalytic activity for PMS activation, leading to complete atrazine degradation in just 4 min (Afzal et al. 2025). Beyond photocatalysis, bimetallic biochar composites, specifically Fe–Mn systems, can effectively activate persulfate (PS) for radical-based atrazine degradation. Liang et al. (2024) found that Fe–Mn bimetallic biochar achieved atrazine removal rates 2.2–2.9 times higher than monometallic biochar, attributed to the synergistic activation of PS and the generation of various reactive oxygen species. Co-pyrolysis strategies can also enhance biochar's inherent properties. Song et al. (2024) showed that co-pyrolyzing macroalgae with oyster shells produced nitrogen-doped porous biochars with exceptionally high surface areas (up to 1501.8 $m^2$ $g^{-1}$) and atrazine sorption capacities reaching 340.5 mg $g^{-1}$. Furthermore, Yang et al. (2018) found that corn-straw-derived biochar colloids at 700 °C displayed an impressive atrazine adsorption capacity of 139.3 mg $g^{-1}$. This emphasizes the essential role of biochar preparation methods in optimizing its performance. These diverse approaches, detailed in the following table, illustrate the potential for creating highly effective and tailored biochar-based materials for atrazine remediation.

## 4 Engineering biochar for ep removal using artificial intelligence

The transition from lab-scale synthesis of tailored biochar composites to their effective, large-scale application is a complex optimization challenge. Traditional biochar design has largely relied on empirical, trial-and-error strategies in which material selection and optimization are guided by isolated experiments rather than systematic prediction (Zhao et al. 2025). Although this approach has produced valuable insights, it is time- and resource-intensive and often fails to capture the complex, multivariable interactions governing EP adsorption, especially when synthesis parameters such as temperature and residence time are adjusted using one-variable-at-a-time (OVAT) methods. To address these limitations, artificial intelligence (AI) and machine learning (ML) offer powerful alternatives by leveraging algorithms such as artificial neural networks (ANNs), support vector machines (SVMs), and random forests (RF) to model the intricate relationships across the biochar lifecycle, thereby accelerating optimization and enabling pollutant-specific material tailoring previously unattainable through conventional approaches (Gupta et al. 2023).

Before modelling the complex interactions with pollutants, AI must first be used to optimize the foundational step: the biochar production process itself. Early models focused on predicting key characteristics like yield, elemental composition, and surface properties (Supraja et al. 2023). For well-defined systems with narrow datasets, traditional statistical models like response surface methodology (RSM) have proven highly effective. In fact, one study modelling biochar yield from palm kernel shells with only 17 experimental runs found that an RSM quadratic model ($R^2 = 0.99$) outperformed an ANN model ($R^2 = 0.90$) (Sait et al. 2025). This indicates that for optimizing a limited set of variables, complex ML models may not always be necessary. However, the true power of ML is unleashed when dealing with larger, more diverse, and incomplete datasets aggregated from literature, where conventional methods are inadequate. By leveraging data from dozens of studies, ML can guide the logical design of novel materials. For instance, one study utilized RF and gradient boosting regression (GBR) models trained on 169 data points from 39 different feedstocks to predict the specific surface area (SSA) and total pore volume (TPV) of biochar (Li et al. 2023b). The model not only identified pyrolysis temperature, biomass ash, and volatile matter as key predictors but was also used to optimize biomass mixing ratios, resulting in a composite biochar with significantly improved SSA (by > 40%) and TPV (by > 85%) compared to biochars from single feedstocks. This ability to reliably predict and engineer fundamental properties from varied process parameters forms the critical foundation for a targeted, "design-by-prediction" approach for creating effective adsorbents.

### 4.1 Predictive modelling for pollutant removal

Building on the ability to predict intrinsic biochar properties, the next frontier for AI is forecasting pollutant removal performance. To date, the most comprehensive ML applications have focused on the adsorption of heavy metals and other inorganic pollutants, providing a valuable blueprint that can be adapted for EPs. For example, in a study using 528 data points from 61 different biochars, ML algorithms like RF, SVR, and XGBoost were used to predict the adsorption capacity for emerging inorganic pollutants (Ullah et al. 2025). The XGBoost model proved most efficient ($R^2 = 0.90$), identifying reaction pH, biochar dosage, and pyrolysis temperature as the most critical predictors from a wide array of inputs spanning synthesis conditions, biochar properties, reaction conditions, and pollutant properties. However, the key features and underlying mechanisms governing heavy metal removal are not directly transferable to the structurally diverse class of organic EPs. For instance, studies on multivalent cationic metals often find that biochars with low

carbon content (< 20%) and high ash content exhibit the highest adsorption capacities (> 500 mg $g^{-1}$), while surface area has a negligible effect (Shanmughan et al. 2025). This is because removal is dominated by mechanisms like electrostatic adsorption, functional group complexation, ion exchange, and precipitation. This contrasts sharply with many EPs, where high carbon content, large surface area, and hydrophobicity are paramount for mechanisms like π–π interactions and pore-filling.

AI is also proving invaluable for modelling the removal of specific, high-profile organic EPs, though applications in this area are still emerging and often rely on limited, lab-generated data. For instance, in a study targeting PFOA removal, ANN and adaptive neuro-fuzzy inference system (ANFIS) models were used to predict its adsorption onto magnetic biochar with extremely high accuracy ($R^2 > 0.99$). The models successfully identified optimal conditions achieving over 98% PFOA removal but were developed from a small dataset of just 19 experimental runs (Saawarn et al. 2024). Similarly, ANN and ANFIS models have been used to precisely predict the removal of the pesticide chlorpyrifos based on batch experiments (Bisaria et al. 2024). While these studies validate the precision of AI, their reliance on small datasets highlights that this is a growing field requiring a larger, more diverse database of experimental data to build truly robust and generalizable models for the vast array of EPs. Beyond predicting batch adsorption, AI also shows great promise for optimizing more complex systems and providing economic benefits. An ANN model trained on 768 data points successfully predicted the dynamic adsorption of pollutants in a fixed-bed column (Zhao et al. 2025), demonstrating AI's capability to model continuous-flow systems that mimic industrial applications. Furthermore, coupling a predictive model with optimization algorithms can yield significant cost savings, as shown in a study that used an ANN to optimize the photocatalytic degradation of 2,6-dichlorophenol, resulting in a 16% reduction in total treatment cost (Alhajeri et al. 2024).

### 4.2 Considerations for successful AI implementation in EP removal

#### *4.2.1 Data retrieval and feature engineering*

The success of any predictive model hinges on the quality and breadth of its training data. For AI to effectively guide the design of biochar for EP removal, it requires large, multidimensional datasets, with studies often utilizing hundreds of data points to achieve high accuracy (Zhao et al. 2025; Shanmughan et al. 2025). Based on data from the earlier sections, the necessary input variables, or features, can be grouped into five key categories (Table 4): (1) feedstock properties (e.g. proximate, ultimate, and biochemical composition); (2) pyrolysis conditions (temperature, heating rate, residence time); (3) biochar properties (e.g. surface area, pore characteristics, pH, zeta potential, elemental ratios); (4) system conditions (e.g. adsorbent dose, initial pollutant concentration, solution pH); and (5) pollutant properties (e.g. molecular weight, pKa, log Kow, molecular dimensions). These comprehensive descriptors enable a

**Table 4** Key input variables for ML models in biochar-based EP remediation

| Category | Input variable | Rationale and importance for EPs |
|---|---|---|
| Feedstock properties | Proximate Analysis: Ash, Volatile Matter, Fixed Carbon | Ash content influences surface mineralogy and pH, affecting electrostatic interactions |
| | Ultimate Analysis: C, H, N, O, S | Indicator for potential heteroatom doping, creating active sites for catalysis and polar interactions |
| | Biochemical: Cellulose, Hemicellulose, Lignin | Lignin content correlates with higher aromaticity in the final biochar, promoting *π–π* interactions with EPs like pharmaceuticals |
| Pyrolysis conditions | Temperature, Heating Rate, Residence Time | Controls carbonization, pore development, functional group retention |
| Biochar properties | Physical: BET Surface Area, Pore Volume, Pore Size | Governs hydrophobicity, electrostatic potential, and site availability |
| | Chemical: pH, pHpzc, CEC, Elemental Ratios (O/C, H/C) | pHpzc determines surface charge and is critical for the electrostatic adsorption of charged EPs (e.g., PFAS, ionized pharmaceuticals) |
| System conditions | Adsorbent Dose, Initial EP Conc., Solution pH, Temp | Solution pH controls both the biochar surface charge and the speciation (charge) of the EP, dictating the dominant interaction mechanism |
| Pollutant properties | Molecular Weight & Size | Directly impacts diffusion into pores and steric hindrance |
| | pKa | Determines the charge of the EP at a given pH, influencing electrostatic attraction/repulsion |
| | log Kow (Octanol–Water Partition Coefficient) | A key indicator of hydrophobicity, predicting the strength of hydrophobic interactions with the biochar surface |
| | Molecular Structure | Presence of aromatic rings, functional groups (e.g., –COOH, –F, $–NH_2$), and molecular charge are critical for predicting mechanisms like *π–π* stacking, hydrogen bonding, and fluorous interactions |

model to not only generalize across diverse EP classes but also to identify design rules for tailoring biochar to target specific removal mechanisms like electrostatic attraction, π–π stacking, or hydrophobic partitioning. A prime example of this directional construction was a study that used ML to predict biochar's N-content (Leng et al. 2022), a property integral to the removal of certain EPs like PFAS via amine groups (He et al. 2024). Using a large dataset of 400 biochar samples derived from 64 different feedstocks, a multi-target GBR model was trained with 14 input variables spanning the feedstock's elemental, proximate, and biochemical composition, alongside pyrolysis conditions (Leng et al. 2022). The model successfully predicted N-content ($R^2$ in the range of 0.90–0.95) and identified biomass N and ash content as the most influential factors, providing a clear recipe for engineering N-rich biochars.

Interestingly, while material properties are crucial, several large-scale AI studies have revealed that experimental and system conditions can be even more influential in determining the final removal efficiency. In one study predicting ammonia nitrogen adsorption across 417 datasets and 46 distinct biochar types, it was found that experimental conditions accounted for 67% of the performance variation, while the material's chemical and physical properties contributed only 18% and 15%, respectively (Liu et al. 2025a). Another comprehensive study using 770 data samples and 8 ML models to predict ammonia nitrogen adsorption similarly found that the XGBoost model ($R^2 = 0.98$) identified biochar dosage, adsorption time, initial concentration, and solution pH as the most integral variables, superseding many intrinsic material properties (Xie et al. 2025). This underscores the critical importance of including system parameters in any predictive model to ensure its real-world relevance. Looking forward, to elevate predictive power from forecasting performance to truly modelling mechanisms, the field must transition from using bulk properties (e.g., total N-content) to more granular, surface-specific features. Future advanced models will depend heavily on the creation of large datasets from characterization techniques like X-ray Photoelectron Spectroscopy (XPS), which can distinguish between specific functional groups (e.g., pyridinic-N vs. pyrrolic-N), and Raman spectroscopy, which can quantify structural defects. Incorporating these features will be key to unlocking the next level of precision in AI-guided biochar design.

#### *4.2.2 Data preprocessing*

Given that datasets are often aggregated from diverse literature sources, a multi-step preprocessing workflow is essential to ensure consistency and prevent errors. For example, it's essential to verify the basis on which compositional data is reported; proximate analysis should be standardized to a dry basis (where Volatile Matter + Ash + Fixed Carbon ≈ 100%), and elemental composition to a dry, ash-free basis (where C + H + N + S + O ≈ 100%) (Li et al. 2023b). Failing to harmonize these reporting standards can introduce significant, systemic errors before model training even begins. Beyond this, a primary challenge is handling missing values. Common approaches range from simple elimination of incomplete entries to more sophisticated methods like median imputation (Xie et al. 2025) or using the K-nearest neighbors (KNN) algorithm (Liu et al. 2025a) to infer values based on the most similar samples in the dataset. Next, raw data must be transformed. Categorical features are recoded into numerical forms using tools like LabelEncoder, while numerical data is normalized to prevent features with large absolute values from biasing the model (e.g., surface area in hundreds of $m^2\ g^{-1}$ vs. H/C ratio < 1) (Ullah et al. 2025). This is typically achieved via Z-score normalization or by scaling all variables to a common range (Xie et al. 2025). Finally, transformations like the Box-Cox transformation can be applied to stabilize variance and handle data that does not follow a normal distribution, improving the model's fit and predictive accuracy (Liu et al. 2025a).

Once the data is cleaned and standardized, the next phase involves feature selection and model building. It's a common misconception that more input variables lead to a better model; in fact, redundant or irrelevant features can weaken a model's generalization ability and increase computational cost (Leng et al. 2022). Therefore, an iterative process of feature selection is often employed. Techniques like Pearson Correlation Coefficient (PCC) analysis are used to identify and remove variables that are highly correlated with each other (multicollinearity) (Liu et al. 2025a). The refined dataset is then typically split, with 80–90% used for training the model and the remaining reserved for testing its performance on unseen data.

*Model development and interpretation.*

After data preprocessing, a crucial step is selecting the appropriate ML model. The choice depends on the dataset's size and complexity, but studies consistently show that tree-based ensemble models (RF, GBR, XGBoost, LightGBM, and CatBoost) are exceptionally effective for biochar's tabular data (Liu et al. 2025a; Ullah et al. 2025), compared to single-model (SVR, SVM, KRR and GRP) and deep-learning (CNN, ANN, and LSTM) approaches (Fig. 6A). These ensembles, which combine multiple "weak learners" into one strong model perform better for a number of reasons: Leng et al. (2024) found that RF better predicted nitrogen functional groups ($R^2 = 0.91–0.97$) owing to its resistance to overfitting and robustness against noisy data; Zhou et al. (2024) and Liu et al. (2025b) demonstrated that XGBoost and CatBoost

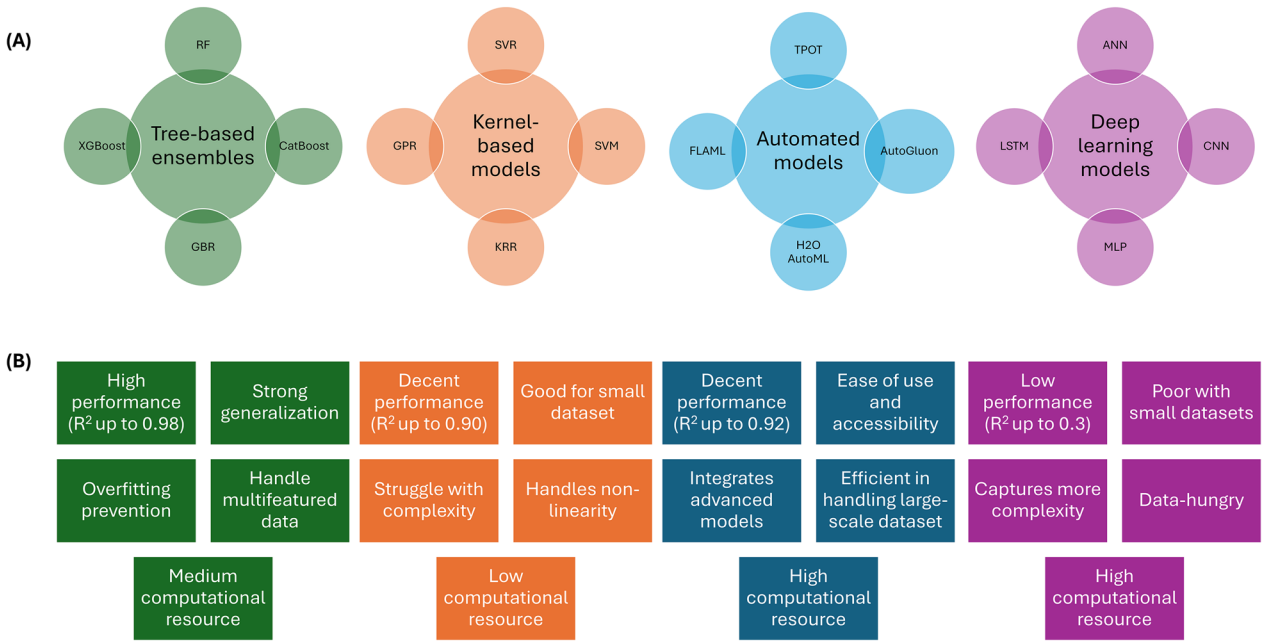


**Fig. 6** **A** Overview of models for AI-driven biochar engineering; **B** AI-guided hybrid framework for predictive design and engineering of biochar for EP adsorption. The framework integrates four iterative stages, enabling continuous feedback and refinement, with the final application aimed at deploying AI-driven decision tools for targeted synthesis and large-scale implementation of high-performance biochars for EP removal

provide the best balance between precision and generalization, with test $R^2$ values up to 0.92–0.97 for yield and surface area, owing to their built-in regularization and ability to handle missing data. On the other hand, Deep learning models such as CNN and LSTM underperformed ($R^2 < 0.3$) when applied to limited datasets, confirming that such architectures require much larger, high-dimensional data to be effective (Liu et al. 2025a). Other models like SVR are useful for small, non-linear samples (Xie et al. 2025). Automated ML frameworks (e.g., H2O AutoML, AutoGluon, FLAML) have recently emerged to streamline hyperparameter tuning and model selection, achieving prediction accuracies near $R^2 = 0.92$ (Wang et al. 2025b). Together, these findings suggest that ensemble-based methods remain the most reliable for current-scale biochar data, while automated ML and hybrid deep-learning pipelines hold promise for future large-scale predictive frameworks.

The final and most important step is model interpretation, which transforms the model's predictions into scientifically meaningful insights. Performance is first quantified using statistical metrics like the coefficient of determination ($R^2$), root mean squared error (RMSE) and mean absolute error (MAE) (Ullah et al. 2025). Beyond accuracy, tools like SHAP (SHapley Additive exPlanations) and partial dependence plots (PDPs) are used to understand the model's behaviour (Xie et al. 2025). These methods rank the feature importance, revealing which input variables have the most significant impact on the adsorption capacity. This process is often iterative; features identified as having low importance may be removed in subsequent model-building rounds to create a more efficient and robust predictive tool. Figure 6B provides a framework for engineering biochar for EP removal, adapted from Leng et al. (2025) for metal adsorption using biochar. The framework is one of the first to integrate three models to create a direct link from raw biomass and pyrolysis conditions to final EP removal performance, enabling directional design and optimization.

### 4.3 Future outlook and key research directions in AI-driven biochar engineering

Despite its immense potential, the successful application of AI for designing biochar-based EP removal technologies is not without its challenges, which in turn define future research directions. The primary bottleneck is data scarcity and heterogeneity. The predictive power of any ML model is fundamentally dependent on the quality, quantity, and diversity of the data it is trained on (Zhao et al. 2025; Ullah et al. 2025). While successful models have utilized hundreds of data points, a significant hurdle remains: the lack of standardized reporting in the literature, which makes data aggregation difficult and unreliable (Kumari et al. 2024). To build the robust and generalizable models needed to advance the field, future research must be underpinned by a community-wide

effort to establish an open-source database governed by a standardized data reporting template. This would ensure all key variables (e.g. feedstock composition to pollutant properties and system conditions) are consistently captured, creating the high-quality datasets necessary for the development of powerful and reliable predictive tools.

A second major challenge is bridging the lab-to-pilot gap. The vast majority of data currently available for training AI models is derived from small-scale batch experiments conducted under idealized laboratory conditions (Xie et al. 2025; Shanmughan et al. 2025; Leng et al. 2025). For example, in one study an RF model had significantly higher prediction accuracy for lab-scale ($R^2$ up to 0.87) compared to pilot scale ($R^2$ up to 0.65) (Cheng et al. 2020). While essential for fundamental understanding, these conditions do not reflect the complexities of real-world water treatment, which often involves continuous-flow systems and dynamic influent concentrations. Consequently, models trained exclusively on batch data may have limited utility in predicting performance at a larger scale. A concerted research effort is therefore required to generate comprehensive datasets from continuous-flow column studies and pilot-scale systems. Finally, current models exhibit limited transferability to real-world scenarios due to their focus on single-pollutant systems. Wastewater is invariably a complex mixture of co-contaminants, where competitive or synergistic adsorption effects can significantly alter biochar performance in ways that are not captured by single-EP models (Satyam and Patra 2024). Future research must increasingly focus on generating data from experiments with complex, multi-pollutant matrices to train models that can navigate these interactions. This will allow for the development of more sophisticated AI tools capable of designing biochar adsorbents that are not only effective but also highly selective.

## 5 Scalability of biochar composites for EP removal: environmental and economic considerations

While the preceding sections have demonstrated the impressive performance of engineered biochar, its practical implementation is ultimately governed by real-world scalability and viability. The feasibility of producing consistent biochar quality at scale has already been demonstrated, with similar properties achieved at production scales ranging from the lab up to 100 kg. However, successful deployment requires a holistic assessment of the associated economic and environmental trade-offs (Mašek et al. 2018). To provide this analysis, this section reviews key findings from techno-economic analysis (TEA) and life-cycle assessment (LCA) studies. Central to any such assessment is a clearly defined system boundary, such as the 'cradle-to-grave' framework illustrated in Fig. 7, and a consistent functional unit. For this review, the functional unit is defined as 'the production of 1 ton of biochar material suitable for water treatment'. Therefore, this section focuses on the economic considerations, the environmental footprint, and the ecotoxicological concerns of both pristine and composite biochar systems. Finally, a dedicated subsection addresses adsorbent regeneration and end-of-life management.

### 5.1 Economic considerations

A comprehensive systematic review by Campion et al. (2023) established that the profitability of biochar production is highly context-dependent, influenced by geographical location, feedstock availability, production scale, process parameters, and market pricing. Within a cradle-to-grave system boundary, these variables collectively determine whether biochar can achieve favourable life-cycle returns when co-products, such as heat and syngas, are valorised. For instance, a study that evaluated the possibility of integrated biochar production and heat generation in Ecuadorian industries producing quinoa and lupin waste residues revealed that the heat generated from the carbonization process exceeded the thermal energy needed for saponins removal (Salgado et al. 2018). To elucidate these dynamics, techno-economic studies have examined biochar systems under varying location, feedstock, and process scenarios.

#### *5.1.1 Scenario 1: location-dependent cost variations*

Production costs and economic feasibility differ significantly between the Global North and Global South due to differences in feedstock availability, labour cost, and energy demand. Studies in Asia have reported profitable biochar production with selling prices reaching < 200 USD per ton. For instance, Hu et al. (2024) reported that large-scale biochar production from swine manure in China (8000 tons capacity per year) achieved a viable internal rate of return (11%) at a selling price of 154 USD per ton, with a payback period of 4.6 years, and that a positive net present value was achieved only when biochar price was over 116 USD per ton. Similarly, Pandit et al. (2018) estimated a minimum selling price (MSP) of 144 USD per ton for biochar derived from Nepalese agro-residues, reflecting low input costs and decentralized small-scale operations.

In contrast, cost models incorporating U.S.-based conditions, characterized by higher labour costs, stricter emission compliance, and more expensive logistics, show substantially higher MSPs. Comparative data (Fig. 8A, B) revealed that for similar crop residue feedstocks, the

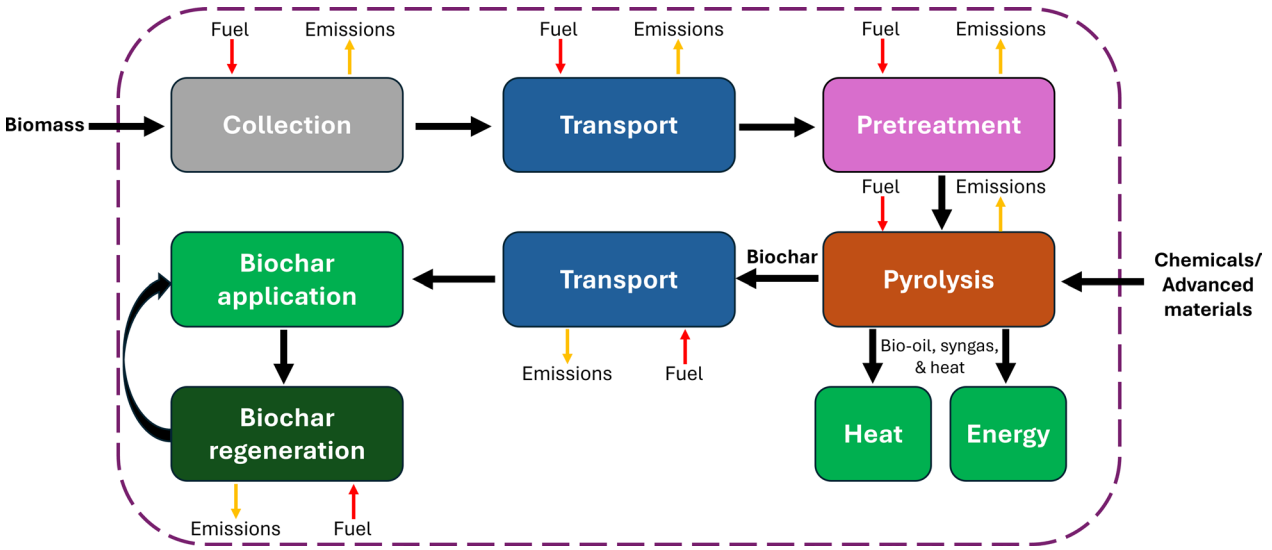


**Fig. 7** A cradle-to-grave system boundary for biochar production and application

MSP in China was approximately 270.5 USD per ton (resulting in a net profit of nearly $47 USD per tonne) (Yang et al. 2021), whereas in the United States it reached 1100 USD per ton (Cheng et al. 2020). This nearly four-fold disparity highlights how local resource costs, energy prices, and transportation distances critically shape the economic outcomes of biochar production within cradle-to-grave boundaries.

#### *5.1.2 Scenario 2: feedstock-based trade-offs*

Feedstock type strongly influences both the production cost and life-cycle performance of biochar. Sludge and manure-derived biochars are often more economically favourable due to low or zero feedstock acquisition costs, many wastewater utilities and livestock farms provide these residues freely for waste management purposes (Rajabi Hamedani et al. 2019). In contrast, crop residues and woody biomass possess competing market values (as soil amendments or fuel), elevating procurement costs.

Quantitatively, sludge biochar pyrolyzed between 400–700 °C exhibited an MSP ranging between 700–1000 USD per ton, while crop- and wood-derived biochars reached up to 1400 USD per ton under comparable operating conditions (Fig. 8B). The cost advantage of sludge is partially due to higher char yield, attributed to its elevated ash content. As shown in Fig. 8C, at 700 °C, annual sludge biochar output reached 18.7 kt, compared to 16.8 kt for crop residues and 14.8 kt for woody biomass (Cheng et al. 2020). Although sludge requires more drying energy, raising its global warming potential (GWP), the reduced feedstock cost and higher yield often offset this drawback within the techno-economic balance (Rajabi Hamedani et al. 2019; Karadirek et al. 2025).

When large farms or agro-industries reuse their own residues as feedstock, the need for external procurement is eliminated, further reducing production costs and improving net life-cycle benefits. Integrating renewable drying technologies, particularly solar drying, offers an additional opportunity for cost optimization (Bennamoun 2012). In a techno-economic study using date palm biomass, switching from conventional to solar energy for drying increased profits from 450 to 480 USD per ton of biochar, while reducing production costs from 1060 to 1040 USD per ton of biochar (Shaheen et al. 2022). Such renewable-energy integration is particularly viable in hot, high-irradiation regions like the Gulf.

Moreover, even when the drying phase of sludge pyrolysis is considered, the life-cycle cost remains lower than alternative waste management options. A Canadian case study found that pyrolysis of sewage sludge resulted in at least 27% lower life-cycle cost per ton compared to incineration or anaerobic digestion (Zhuang et al. 2022). Therefore, coupling free or low-cost feedstocks with solar-based or waste-heat drying substantially improves the economic performance of biochar systems within cradle-to-grave boundaries, especially in regions where renewable energy is abundant.

#### *5.1.3 Scenario 3: influence of activation*

Activation processes represent one of the most cost-intensive stages within the cradle-to-grave boundary. The production temperature, activating agent, and residence time jointly dictate both material properties, and

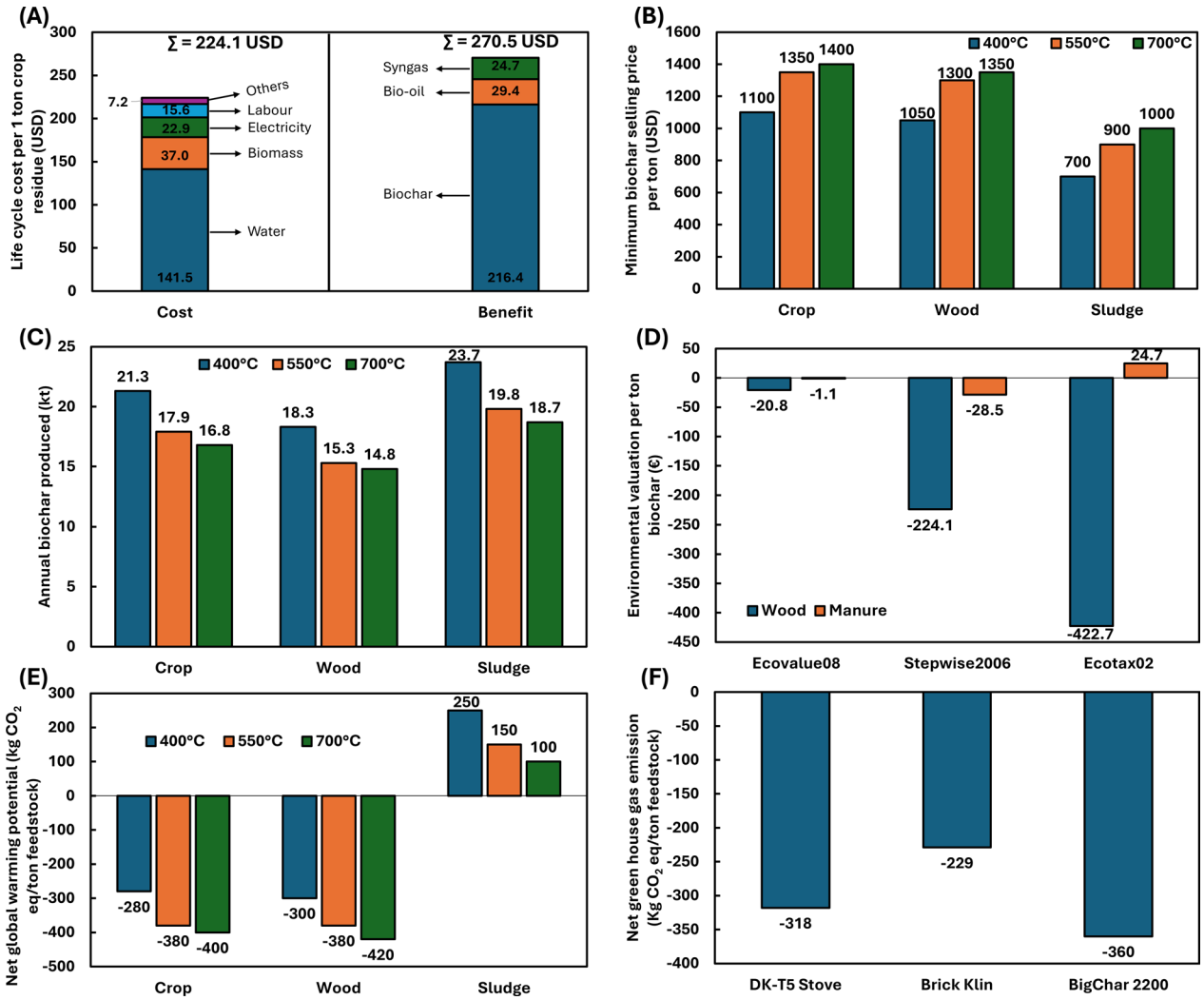


**Fig. 8** Economic profile of biochar production. **A** Life cycle cost and benefit breakdown for producing 1 tonne of crop residue biochar in China. **B** Minimum sustainable selling price (MPSP) for biochar from different feedstocks in the US. **C** Annual biochar yield from a large-scale facility. **D** Environmental valuation per ton of biochar produced using selected valuation tools. **E** Net global warming potential associated with different feedstocks at varying pyrolysis temperatures. **F** Net greenhouse gas emission from different furnaces

the overall techno-economic balance. For example, in one study, date palm biochar production was estimated to cost 1060 USD per ton, while activated carbon production via high temperature (1000 °C) and steam treatment (816–927 °C) resulted in a 26% cost increase (Shaheen et al. 2022). Another study by Jaria et al. (2022) investigated activated carbon production from waste almond shells revealed that conventional pyrolysis (up to 450 °C) with phosphoric acid activation (1:1 w:w ratio) yielded 34–39% product with surface areas of 822–1458 $m^2$ $g^{-1}$, costing approximately 2450–2820 USD per ton (Toles et al. 2000a; Jaria et al. 2022). Higher temperature pyrolysis (up to 800 °C) followed by steam activation, producing yields of 7–16% and specific surface areas of 515–673 $m^2$ $g^{-1}$, cost 1540–1910 USD per ton. $CO_2$ activation under similar pyrolysis conditions achieved comparable SSA (505–560 $m^2$ $g^{-1}$) but increased production costs to 2930 USD per ton, reflecting higher energy demand and lower throughput efficiency (Toles et al. 2000b; Jaria et al. 2022). Particularly costly was $ZnCl_2$ + lime activation of tannery sludge, reaching 70,700 USD per ton (Puchana-Rosero et al. 2016; Jaria et al. 2022).

Overall, activation introduces a trade-off between surface functionality and process cost. The improved surface area and microstructural order from activation typically results in enhanced adsorption kinetics and regeneration efficiency, yielding long-term performance gains that can offset higher initial investment. Moderate-temperature

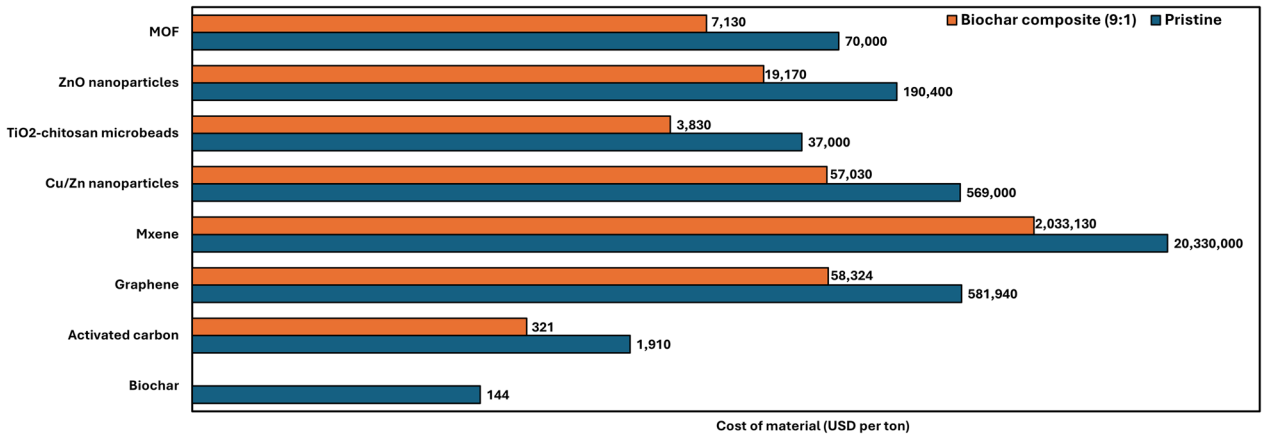


**Fig. 9** Comparative production costs (USD per ton) of different biochar and adsorbent materials. Materials were selected to illustrate the full economic spectrum of adsorbents discussed in this review. This ranges from the low-cost biochar baseline ($144 per ton) and the current industrial benchmark (activated carbon) ($1910 per ton) to the high-cost, high-performance advanced materials (e.g., graphene, MXenes) used in composites

self-activation approaches, such as co-pyrolysis with mineral-rich biomass, present an emerging middle ground, balancing performance with cost and environmental sustainability within system boundaries.

#### *5.1.4 Scenario 4: integration of advanced materials into biochar matrices*

Incorporating advanced materials (e.g., nanoparticles, graphene, MXenes, MOFs) into biochar matrices can drastically elevate performance but also increase the overall cost. Graphene produced from laser-induced graphitization costs 549–1018 EUR per kg, equivalent to ~ 600,000–1,100,000 USD per ton (Jin 2024), while MXenes average 20.33 million USD per ton (Zaed et al. 2024). In contrast, nanoparticle composites exhibit costs between 569,000 USD per tonne for biosynthesized Cu/Zn (Noman et al. 2019) to 37,000 USD per ton for $TiO_2$–chitosan (Meramo-Hurtado and González-Delgado 2020). Similarly, the biosynthesis of ZnO nanoparticles using orange peels and zinc acetate dihydrate was reported at ≈ 190,400 USD per ton, with over 70% of the production cost attributed to the zinc acetate precursor (Yashni et al. 2021). MOFs, depending on synthesis route and metal source, have production costs as high as 70,000 USD per ton (Peng et al. 2024).

Blending small fractions of such materials with biochar drastically reduces total material cost while preserving advanced functionality (Fig. 9). For example, a composite containing 90% biochar (144 USD per ton) and 10% MXenes (20.33 million USD per ton) yields a composite cost of approximately 2.03 million USD per ton, representing an 18-fold reduction compared to pure MXene (Pandit et al. 2018; Zaed et al. 2024). Thus, hybridization enables scalable production of high-performance adsorbents with reduced economic and environmental burdens relative to their pure counterparts.

### 5.2 Environmental considerations

The large-scale deployment of biochar systems offers considerable potential for GHG mitigation and carbon sequestration. Theoretically, converting all available plant biomass into carbon-dense char could withdraw up to 90 Gt $CO_2$ from the atmosphere, approximately one-quarter of carbon fixed via photosynthesis (Wang et al. 2013). Beyond carbon capture, large-scale biochar production also supports EP degradation during pyrolysis. For instance, biosolids from municipal wastewater treatment containing PFAS, microplastics, and PPCPs achieved > 99% removal after pyrolysis (Keller et al. 2024). Within a cradle-to-grave framework, the environmental impact depends on factors like production scope, feedstock type, pyrolysis scale and technology, and incorporation of advanced materials. Accordingly, four distinct scenarios are analyzed in this section.

#### *5.2.1 Scenario 1: on-site (decentralized) versus centralized biochar production*

The environmental impact of biochar production is highly dependent on the degree of decentralization and the proximity between feedstock source, processing facility, and application site. A UAE life-cycle study on date-palm biochar found that feedstock transport (54.6 km) and product delivery to wastewater plants (39.1 km) were major contributors to the ionizing-radiation impact (40%) (Shaheen et al. 2022). Sensitivity analysis revealed that reducing transport distances to 20 km (feedstock) and 10 km (product) reduced the GWP from 1.53 to 1.29 kg $CO_2$ -eq $kg^{-1}$. Similarly, a China-wide assessment

(Fig. 8B) showed that biomass transportation was the third highest source of carbon emission (4.09 × 107-ton $CO_2$ -eq), substantially contributing to all environmental impact categories (Yang et al. 2021).

By contrast, on-farm or regional pyrolysis hubs drastically reduce logistics-related burdens. The Taihu Lake farm network model exemplified this: farmers converted rice, wheat, and mushroom residues into biochar at 500 °C, achieving 25–35% yields, while using biogas generated on-site to sustain both pyrolysis and farm heating (Wang et al. 2013). This closed-loop system achieved near energy self-sufficiency, eliminated transport-related GHG emissions, and improved nutrient recycling (Fig. 10). Consequently, although centralized pyrolysis facilities may achieve economies of scale, their benefits are often outweighed by transport-induced emissions and energy requirements.

#### *5.2.2 Scenario 2: influence of pyrolysis equipment*

The environmental outcomes of biochar production are strongly influenced by the design and efficiency of pyrolysis equipment. Systems that enable complete recovery of co-products (bio-oil, syngas, and heat) significantly outperform traditional configurations in cradle-to-grave assessments. The value-added utilization of bio-oil and syngas can offset fossil fuel consumption and substantially lower life-cycle emissions; however, in traditional earthen or brick kilns, these products are often vented or flared due to equipment limitations (Zhu et al. 2022). For example, orange peel pyrolyzed at 740 °C generated 50% tar, 28% biochar, and 22% syngas, all contributing to internal energy recovery (Negro et al. 2017). Comparative field studies show that household DK-T5 stoves, which utilize partial gas recirculation, achieved $-318 \pm 174$ kg $CO_2$ -eq $t^{-1}$ biomass, while village-level brick kilns, where no energy recovery occurs, exhibited a smaller reduction of $-229 \pm 91$ kg $CO_2$ -eq $t^{-1}$ (Mohammadi et al. 2017). Conversely, large-scale BigChar 2200 units integrated with heat exchangers achieved $-360 \pm 144$ kg $CO_2$ -eq $t^{-1}$, demonstrating that efficient gas and heat utilization dictates environmental performance.

Equipment design also influences primary emission intensity. Commercial dual-auger units processing 380 kg $h^{-1}$ of woody biomass produced 63 kg $h^{-1}$ of biochar with power consumption of 4.5 kW, but emitted 160 g CO, 120 g propane, 51 g $NO_x$, and 43 g $SO_2$ $h^{-1}$, along with 380 g $h^{-1}$ of particulates (Severy et al. 2018). Employing advanced designs such as two-box chamber pyrolyzers significantly mitigates these releases; processing 1.5 kg oil-palm frond at 500 °C for 30 min yielded a GWP of 1.35 kg $CO_2$-eq $kg^{-1}$, which was 21% lower than

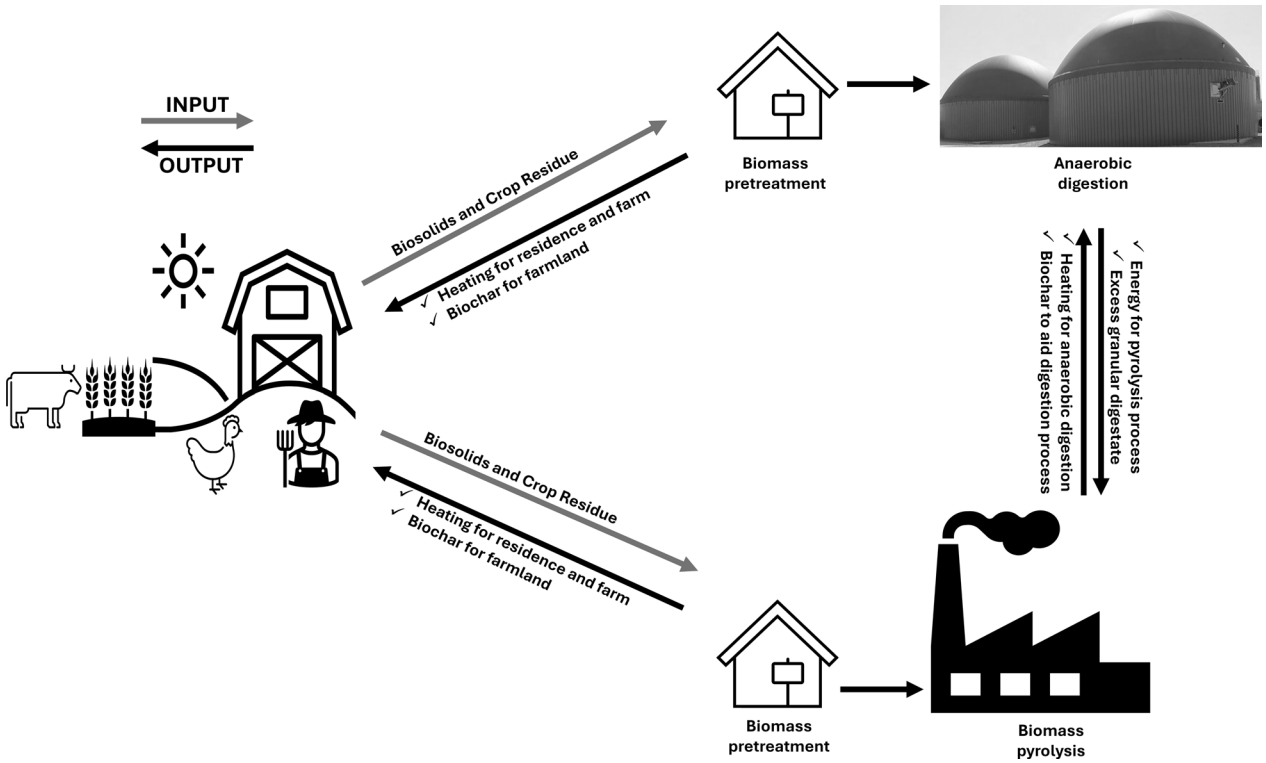


**Fig. 10** Sustainable large-scale biochar production integrating circular economy approach

conventional pyrolysis and 53% lower than natural composting (Bindar et al. 2024). Collectively, these results confirm that the integration of energy recirculation and emission control systems can reduce GWP by up to 40%, transforming pyrolysis from a simple carbonization process into a closed-loop waste-to-energy platform.

#### *5.2.3 Scenario 3: feedstock-specific environmental dynamics*

Feedstock type introduces trade-offs between energy efficiency, drying demand, and carbon sequestration. Sludge and manure biochars generally have higher moisture contents (~80%) and lower fixed-carbon fractions, leading to greater energy consumption and positive GWP contributions (Zhuang et al. 2022; Li et al. 2024a). Comparative LCA data show that sludge systems often remain net-positive emitters, whereas lignocellulosic biomass (moisture ≈ 20%) achieves net-negative GWPs due to higher carbon content and energy co-recovery (Cheng et al. 2020). At 400, 550, and 700 °C, increasing temperature enhances carbon stabilization in lignocellulosic chars, raising retained biochar carbon (kg C $kg^{-1}$ char) and yielding progressively lower GWP values (Cheng et al. 2020).

Figure 8D compares environmental monetary valuation between wood- and manure-derived biochars, showing that wood biochar achieved −224 to −423 EUR $t^{-1}$ under Stepwise 2006 and Ecotax02 models, while manure ranged −29 to +25 EUR $t^{-1}$ due to high drying energy (Rajabi Hamedani et al. 2019). Figure 8E similarly illustrates that the GWP of willow biochar (−2063 kg $CO_2$ -eq $t^{-1}$) far outperforms pig-manure biochar (−472 kg $CO_2$ -eq $t^{-1}$), confirming that lignocellulosic feedstocks deliver superior environmental returns when energy co-products are recovered (Rajabi Hamedani et al. 2019). Hence, from a cradle-to-grave standpoint, feedstocks with lower inherent moisture and higher carbon density produce the most sustainable biochar systems.

#### *5.2.4 Scenario 4: environmental implications of using advanced materials*

While coupling biochar with advanced materials, such as nanoparticles, MXenes, graphene, or MOFs enhances adsorption performance, these additives significantly alter the life-cycle footprint. Production of MXenes involves etching precursors with HF or LiF–HCl, contributing to high acidification potential and human toxicity indicators (Alyasi et al. 2024). Similarly, nanoparticle synthesis through sol–gel or hydrothermal routes exhibits large energy intensities (Mpongwana and Rathilal 2022) and generates solvent emissions including ethanol and propanol (Meramo et al. 2018). LCAs have estimated Ag nanoparticle (AgNP) synthesis via flame spray pyrolysis at 1951 kg $CO_2$ -eq $kg^{-1}$ AgNPs (Temizel-Sekeryan and Hicks 2020), whereas emerging green routes drastically lower this impact. Han et al. (2025) reported that bio-based AgNP synthesis using leaf extracts or bacterial reduction reduced GWP to 472–534 kg $CO_2$ -eq $kg^{-1}$, nearly threefold lower than conventional methods, with additional 28–74% reductions achievable when substituting mined silver with recycled silver (Han et al. 2025).

Comparable improvements have been observed for metal oxide nanoparticles, particularly $TiO_2$, widely used for photocatalytic enhancement in biochar matrices. Rodríguez-Rojas et al. (2024) compared conventional chloride-route $TiO_2$ synthesis with a green aqueous route using *Cymbopogon citratus* (lemongrass) extract as the reducing and stabilizing agent. The green method achieved higher yield (92% vs. 74%), shorter reaction time (3 h vs. 3.25 h), and lower production cost (83.6 vs. 88.88 units), translating into reduced energy use and GHG emissions. Critically, it avoided toxic by-products such as hydrochloric acid generated in the chloride route, thus eliminating acidification and ecotoxicity concerns (Rodríguez-Rojas et al. 2024). Integrating such green-synthesized nanoparticles into biochar composites can substantially reduce environmental intensity while retaining functionality.

### 5.3 Regeneration and reusability

End-of-life management is a critical factor in the overall TEA and LCA of an adsorbent, with effective regeneration offering significant economic and environmental benefits. Regeneration costs for activated carbon, for example, are estimated to be \$0.70–\$0.85 USD $kg^{-1}$, which is substantially lower than the production cost of \$0.70–\$1.50 USD $kg^{-1}$ (Harry Marsh and Francisco Rodriguez-Reinoso 2012). This cost-saving principle is even more pronounced for engineered materials; one analysis of an Fe-modified biochar system for wastewater treatment found that incorporating three regeneration cycles increased the daily $CO_2$ emission reduction from ~36,000 to ~38,000 kg $CO_2$ -eq $day^{-1}$ and provided a massive cost reduction of 56,680 USD $day^{-1}$ compared to conventional chemical treatment (Zhang et al. 2025). However, like activated carbon, biochar and nanomaterials typically experience performance losses after 3–5 cycles due to active site blockage, pore collapse, or surface oxidation (Singh et al. 2021b; Yan et al. 2022). The extent of degradation depends strongly on the adsorption mechanism; materials dominated by physisorption tend to regenerate more effectively than those governed by chemisorption, where pollutant-surface bonds are difficult to break (Baaloudj et al. 2025).

The choice of regeneration method is highly dependent on the adsorbent material and pollutant. Conventional methods like solvent washing (e.g., with acetonitrile)

can achieve high desorption rates (> 95%) but merely transfer the pollutant to a new liquid phase, requiring further treatment (Acevedo-García et al. 2020). Alkaline regeneration (0.1 M NaOH) offers a good balance between recovery efficiency and material integrity for metal-doped biochars, while acidic treatments often corrode catalytic sites, diminishing metal ion uptake (Yan et al. 2022). Heat-activated persulfate regeneration has emerged as a robust and scalable option, maintaining ~ 98–99% efficiency across five cycles while simultaneously degrading residual pollutants and minimizing chemical consumption (Baaloudj et al. 2025). In comparison, thermal regeneration can enhance biochar's specific surface area and create new active sites, yielding up to 3.5-fold improvement in adsorption capacity but with partial mass loss (Greiner et al. 2018). For nanomaterials such as magnetite or metal oxides, solvent-based desorption, microwave-assisted regeneration, and supercritical fluid techniques are more common but often limited by high energy demand or incomplete desorption (Masuku et al. 2021; Pandit et al. 2025).

Recent developments in electro-Fenton (EF) regeneration represent a significant leap toward circularity. This process integrates adsorption, pollutant degradation, and in-situ regeneration without the need for external oxidants. Studies have demonstrated that Fe-doped and self-catalyzing biochars can sustain nearly 100% removal efficiency over 6 cycles under optimized EF conditions, maintaining structural integrity and avoiding iron leaching (Acevedo-García et al. 2020; Puga et al. 2021). More advanced dual-metal EF systems, such as Fe–Cu–biochar, achieve > 90% regeneration efficiency after 10 cycles while reducing energy consumption by > 70% compared to conventional adsorption–oxidation systems (Ren et al. 2025). These self-regenerative EF systems simultaneously degrade adsorbed pollutants and restore catalytic sites, representing the most sustainable route for large-scale water treatment applications.

### 5.4 Ecotoxicity considerations

Despite a general perception of relative safety, the potential ecotoxicity of MXenes, remains a significant concern. In one study, MXene nanosheets were classified as "Practically not toxic" after exposure to zebrafish embryo (Rasheed et al. 2024). However, the authors, cautioned about the possibility of neurotoxic effects upon exposure to higher concentrations in effluents. Studies have demonstrated the toxicological effects of nanoparticles and carbon nanotubes on aquatic life, including fish and daphnia (Taghavi et al. 2013), and have indicated potential links to adverse human health effects such as oxidative stress, carcinogenicity, genotoxicity, and immune toxicity (Singh et al. 2024). The potential for these materials to be released into the environment via the effluent of treated water, often termed "washout," is a particular concern, especially for nanoparticles (Olawade et al. 2024b). While the incorporation of magnetic properties into nanoparticles, such as iron oxide nanoparticles, offers a potential avenue for separation and recovery from treated water, the susceptibility of some magnetic materials to oxidation or other chemical transformations during water treatment processes can compromise their magnetic responsiveness and, therefore, their recoverability (Mpongwana and Rathilal 2022). In contrast to the challenges associated with some advanced materials, the relative ease with which AC and biochar can be regenerated underscores the importance of waste-based AC regeneration (Shah et al. 2023).

The ecotoxicity of graphene-based materials, including graphene nanoparticles and GO, is a growing concern. While their antimicrobial properties are well-documented, with studies reporting toxicity to bacteria (both Gram-positive and Gram-negative) and fungi at concentrations as low as 85 μg $mL^{-1}$ through mechanisms such as physical disruption and oxidative stress (Guo and Mei 2014), their release into the aquatic environment poses potential risks to a wider range of organisms. Adverse effects have been observed in algae, invertebrates, plankton, and fish upon exposure to graphene-based materials (Zhao et al. 2014; De Marchi et al. 2018). In vivo studies using animal models reveal that the toxicity of graphene-based materials is highly dependent on the form and route of exposure. For instance, inhalation exposure of rats to graphene for at least 5 days a week resulted in minimal pulmonary toxicity and negligible effects on body weight, blood chemistry, or bronchoalveolar lavage fluid (BALF) inflammation factors (Shin et al. 2015; Kim et al. 2016). Conversely, intratracheal instillation of functionalized graphene (bearing –COOH, –COH, –NH, –F, and $–NH_2$ groups) induced pulmonary inflammation in rats, with positively charged graphene exhibiting a significant dose-dependent increase in polymorphonuclear leukocytes (Lee et al. 2017). Regardless of the specific form, GBMs have been shown to induce reactive oxygen species (ROS) generation. Exposure to GO at concentrations as low as 10 μg $mL^{-1}$ induced oxidative stress in human epithelial cells, with the effect being dose-dependent (Chang et al. 2011). Numerous other studies have similarly reported dose-dependent cytotoxicity and immunotoxicity in human cells exposed to GO in vitro (Guo and Mei 2014). The potential for these nanomaterials to be transported from WWTPs via effluents and sludge guarantees their eventual release into the environment. For example, the application of sewage sludge containing silver nanoparticles to soil resulted in toxic effects on soil microbes, particularly ammonium-oxidizing

bacteria, and silver uptake by oat roots after an 180-day incubation period (Schlich et al. 2018). The ecotoxicity of metal oxide nanoparticles, like ZnO, is also highly dose-dependent. While low concentrations (e.g., 50 mg $L^{-1}$) of ZnO can enhance seedling growth in hydroponically grown rice plants, higher concentrations (above 100 ppm) inhibit growth, likely due to increased ROS generation (Singh et al. 2018). In general, exposure of plankton to metal oxide nanomaterials demonstrates a strong dose–response relationship (Zhu et al. 2019).

Concerns regarding the potential ecotoxicity of biochar also exist, primarily stemming from the possible leaching of harmful substances, particularly when produced at lower pyrolysis temperatures. A comprehensive review identified potential contaminants in biochar, including heavy metals, dioxins, PFAS, and VOCs (Xiang et al. 2021). The concentration of these contaminants is strongly influenced by the feedstock material and pyrolysis conditions. Selecting relatively benign feedstocks and employing higher pyrolysis temperatures can help to minimize the presence of these undesirable compounds by promoting their decomposition or volatilization. For instance, Godlewska et al. (2022) found that biochar produced from the co-pyrolysis of sewage sludge and plant biomass exhibited lower toxicity compared to biochar derived solely from sewage sludge (Godlewska et al. 2022). Dose-dependent ecotoxicity has also been observed in earthworms exposed to biochar, highlighting the importance of considering the application rate and potential impacts on soil organisms (Jia et al. 2023). In addition to inherent contaminants, the potential toxicity of adsorbed pollutants or incorporated metals in composite biochars must also be considered. Oleszczuk et al. (2013) investigated the ecotoxicity of biochars derived from wheat straw, elephant grass, coconut shell, and wicker, containing varying concentrations of metals and PAHs (Oleszczuk et al. 2013). Observed effects included root growth inhibition in *Lepidium sativum*, microbial growth inhibition, toxicity to *Selenastrum capricornutum*, and mortality in *Daphnia magna*. The study strongly correlated toxicity with the PAH content of the biochar, underscoring the need for thorough safety assessments and the development of appropriate regulatory guidelines (Oleszczuk et al. 2013). Therefore, comprehensive safety evaluations are strongly recommended before the large-scale implementation of any biochar-based remediation process.

## 6 Conclusion

The widespread contamination of global aquatic systems with emerging pollutants (EPs) is an urgent environmental and public health challenge requiring immediate, scalable solutions. This review critically addresses this problem by proposing a practical, tiered 'design-to-deployment' framework for biochar-based technologies. This framework advocates for a pragmatic approach, beginning with Tier 1 (Pristine Biochar) as a low-cost, sustainable first line of defense for less recalcitrant EPs; moving to Tier 2 (Modified Biochar) for enhanced performance via in-situ or ex-situ doping and activation; and culminating in Tier 3 (Advanced Composites), which leverage powerful catalytic and targeted chemisorptive mechanisms for the most persistent compounds. We establish that artificial intelligence (AI) is the key enabling tool for this framework, providing a predictive pathway to accelerate the directional construction of tailored materials and move beyond traditional trial-and-error development. Critically, we integrate this material-centric approach with a holistic scalability analysis, demonstrating how techno-economic (TEA), life-cycle (LCA), ecotoxicological, and adsorbent regeneration considerations must guide the deployment of each tier. This integrated blueprint provides an insightful, forward-looking roadmap for the research community, guiding the development of next-generation water treatment solutions from fundamental material science to responsible, large-scale application.

**Acknowledgements**
The authors appreciate Qatar Environment and Energy Research Institute (QEERI) for technical support and Qatar National Library (QNL)for providing open access funding.

**Author contributions**
All authors contributed to the study conception and scope. Material preparation, data collection, and analysis were performed by Ojima Z. Wada and Khaled A. Mahmoud. The first draft of the manuscript was written by Ojima Z. Wada and all authors commented on previous versions of the manuscript. All authors read and approved the final manuscript.

**Funding**
No funds, grants, or other support was received.

**Data availability**
No primary research results, software or code have been included and no new data were generated or analysed as part of this review.

## Declarations

**Competing interests**
The authors declare no competing interests.

**Author details**
[1]Qatar Environment and Energy Research Institute (QEERI), Hamad Bin Khalifa University, Qatar Foundation, P.O. Box 34110, Doha, Qatar. [2]Division of Sustainable Development, College of Science and Engineering, Hamad Bin Khalifa University, Qatar Foundation, P.O. Box 34110, Doha, Qatar.

Received: 6 August 2025 Revised: 16 December 2025 Accepted: 17 December 2025
Published online: 25 February 2026

## References


Abolore RS, Jaiswal S, Jaiswal AK (2024) Green and sustainable pretreatment methods for cellulose extraction from lignocellulosic biomass and its applications: a review. Carbohydr Polym Technol Appl 7:100396. https://doi.org/10.1016/j.carpta.2023.100396

Abu Hasan H, Muhamad MH, Budi Kurniawan S et al (2023) Managing Bisphenol A contamination: advances in removal technologies and future prospects. Water 15:3573. https://doi.org/10.3390/w15203573

Acevedo-García V, Rosales E, Puga A et al (2020) Synthesis and use of efficient adsorbents under the principles of circular economy: waste valorisation and electroadvanced oxidation process regeneration. Sep Purif Technol 242:116796. https://doi.org/10.1016/j.seppur.2020.116796

Achieng GO, Kowenje CO, Lalah JO, Ojwach SO (2019) Preparation, characterization of fish scales biochar and their applications in the removal of anionic indigo carmine dye from aqueous solutions. Water Sci Technol 80:2218–2231. https://doi.org/10.2166/wst.2020.040

Afzal S, Mehmood A, Jin L et al (2025) Efficiency and mechanism of high surface area mesoporous nanocast NC-LaCoO3 for activating peroxymonosulfate to degrade atrazine in water. Sep Purif Technol 354:128823. https://doi.org/10.1016/j.seppur.2024.128823

Agilandeswari P, Venkateshbabu S, Sarojini G, Rajasimman M (2024) Sustainable development and analysis of a novel bio-derived (biochar) nanocomposite for the remediation of carbamazepine from aqueous solution. Chemosphere 347:140696. https://doi.org/10.1016/j.chemosphere.2023.140696

Ahmaruzzaman Md (2021) Biochar based nanocomposites for photocatalytic degradation of emerging organic pollutants from water and wastewater. Mater Res Bull 140:111262. https://doi.org/10.1016/j.materresbull.2021.111262

Alazmi A, El Tall O, Rasul S et al (2016) A process to enhance the specific surface area and capacitance of hydrothermally reduced graphene oxide. Nanoscale 8:17782–17787. https://doi.org/10.1039/C6NR04426C

Algaradah MM (2024) MXene-based adsorbent materials for pollutants removal from water: current challenges and future prospects. Inorg Chem Commun 161:112113. https://doi.org/10.1016/j.inoche.2024.112113

Alhajeri NS, Tawfik A, Nasr M, Osman AI (2024) Artificial intelligence-enabled optimization of Fe/Zn@biochar photocatalyst for 2,6-dichlorophenol removal from petrochemical wastewater: a techno-economic perspective. Chemosphere 352:141476. https://doi.org/10.1016/j.chemosphere.2024.141476

Alrefaee SH, Aljohani MM, Alatawi ISS et al (2024) Removal of acetaminophen from wastewater using a novel bimetallic La/Th metal-organic framework: kinetics, thermodynamics, isotherms, and optimization through Box-Behnken design. Process Saf Environ Prot 189:1134–1150. https://doi.org/10.1016/j.psep.2024.06.046

Altendji K, Hamoudi S (2024) Visible light–driven photocatalytic degradation of atrazine in aqueous phase: impact of the g-C3N4/TiO2/NiFe2O4 nanocomposite activated by potassium peroxymonosulfate. Environ Sci Pollut Res Int 32:1361–1374. https://doi.org/10.1007/s11356-024-35838-7

Alyasi H, Wahib S, Gomez TA et al (2024) The power of MXene-based materials for emerging contaminant removal from water—a review. Desalination 586:117913. https://doi.org/10.1016/j.desal.2024.117913

Assoumani A, Lestremau F, Ferret C et al (2024) Nation-wide monitoring campaign of 49 biocides and surfactants in surface waters and wastewaters. Sci Total Environ 954:176624. https://doi.org/10.1016/j.scitotenv.2024.176624

Baaloudj O, Chiron S, Zizzamia AR et al (2025) Efficient biochar regeneration for a circular economy: removing emerging contaminants for sustainable water treatment. Colloids Surf, A 705:135730. https://doi.org/10.1016/j.colsurfa.2024.135730

Behnami A, Pourakbar M, Ayyar AS-R et al (2024) Treatment of aqueous per- and poly-fluoroalkyl substances: a review of biochar adsorbent preparation methods. Chemosphere 357:142088. https://doi.org/10.1016/j.chemosphere.2024.142088

Bennamoun L (2012) Solar drying of wastewater sludge: a review. Renew Sustain Energy Rev 16:1061–1073. https://doi.org/10.1016/j.rser.2011.10.005

Bindar Y, Steven S, Kresno SW et al (2024) Large-scale pyrolysis of oil palm frond using two-box chamber pyrolyzer for cleaner biochar production. Biomass Convers Biorefin 14:6421–6434. https://doi.org/10.1007/s13399-022-02842-1

Birer AM, Gözmen B, Sönmez Ö, Kalderis D (2021) Evaluation of sewage sludge biochar and modified derivatives as novel SPE adsorbents for monitoring of bisphenol A. Chemosphere 268:128866. https://doi.org/10.1016/j.chemosphere.2020.128866

Bisaria K, Singh R, Gupta M et al (2024) Novel acoustic-activated alkali-functionalized *Trapa bispinosa* peel biochar for green immobilization of chlorpyrifos from wastewater: artificial intelligence modelling and experimental validation. Biomass Convers Biorefin 14:7763–7782. https://doi.org/10.1007/s13399-022-02898-z

Cai N, Larese-Casanova P (2014) Sorption of carbamazepine by commercial graphene oxides: a comparative study with granular activated carbon and multiwalled carbon nanotubes. J Colloid Interface Sci 426:152–161. https://doi.org/10.1016/j.jcis.2014.03.038

Całus-Makowska K, Grosser A, Grobelak A et al (2024) Kinetic study of the simultaneous removal of ibuprofen, carbamazepine, sulfamethoxazole, and diclofenac from water using biochar and activated carbon adsorption, and TiO2 photocatalysis. Desalin Water Treat 320:100817. https://doi.org/10.1016/j.dwt.2024.100817

Campion L, Bekchanova M, Malina R, Kuppens T (2023) The costs and benefits of biochar production and use: a systematic review. J Clean Prod 408:137138. https://doi.org/10.1016/j.jclepro.2023.137138

Chang Y, Yang S-T, Liu J-H et al (2011) In vitro toxicity evaluation of graphene oxide on A549 cells. Toxicol Lett 200:201–210. https://doi.org/10.1016/j.toxlet.2010.11.016

Chen D, Xie S, Chen C et al (2017a) Activated biochar derived from pomelo peel as a high-capacity sorbent for removal of carbamazepine from aqueous solution. RSC Adv 7:54969–54979. https://doi.org/10.1039/C7RA10805B

Chen J, Zhang D, Zhang H et al (2017b) Fast and slow adsorption of carbamazepine on biochar as affected by carbon structure and mineral composition. Sci Total Environ 579:598–605. https://doi.org/10.1016/j.scitotenv.2016.11.052

Chen Z, Li Y, Cai Y et al (2023) Application of covalent organic frameworks and metal–organic frameworks nanomaterials in organic/inorganic pollutants removal from solutions through sorption-catalysis strategies. Carbon Res 2:8. https://doi.org/10.1007/s44246-023-00041-9

Cheng F, Luo H, Colosi LM (2020) Slow pyrolysis as a platform for negative emissions technology: an integration of machine learning models, life cycle assessment, and economic analysis. Energy Convers Manag 223:113258. https://doi.org/10.1016/j.enconman.2020.113258

Cheng H, Zhang J, Chen Y et al (2022) Hierarchical porous biochars with controlled pore structures derived from co-pyrolysis of potassium/calcium carbonate with cotton straw for efficient sorption of diethyl phthalate from aqueous solution. Bioresour Technol 346:126604. https://doi.org/10.1016/j.biortech.2021.126604

Choi Y-K, Choi T-R, Gurav R et al (2020) Adsorption behavior of tetracycline onto *Spirulina* sp. (microalgae)-derived biochars produced at different temperatures. Sci Total Environ 710:136282. https://doi.org/10.1016/j.scitotenv.2019.136282

Chu G, Zhao J, Huang Y et al (2018) Phosphoric acid pretreatment enhances the specific surface areas of biochars by generation of micropores. Environ Pollut 240:1–9. https://doi.org/10.1016/j.envpol.2018.04.003

Clurman AM, Rodríguez-Narvaez OM, Jayarathne A et al (2020) Influence of surface hydrophobicity/hydrophilicity of biochar on the removal of emerging contaminants. Chem Eng J 402:126277. https://doi.org/10.1016/j.cej.2020.126277

Dang B-T, Gotore O, Ramaraj R et al (2022) Sustainability and application of corncob-derived biochar for removal of fluoroquinolones. Biomass Convers Biorefin 12:913–923. https://doi.org/10.1007/s13399-020-01222-x

De Marchi L, Pretti C, Gabriel B et al (2018) An overview of graphene materials: properties, applications and toxicity on aquatic environments. Sci Total Environ 631:1440–1456. https://doi.org/10.1016/j.scitotenv.2018.03.132

Diao Y, Shan R, Li M et al (2023) Magnetized algae catalyst by endogenous N to effectively trigger peroxodisulfate activation for ultrafast degraded sulfathiazole: radical evolution and electron transfer. Chemosphere 342:140205. https://doi.org/10.1016/j.chemosphere.2023.140205

Ding H, Zhang Z, Li Y et al (2022) Fabrication of novel Fe/Mn/N co-doped biochar and its enhanced adsorption for bisphenol a based on $\pi$–$\pi$

electron donor–acceptor interaction. Bioresour Technol 364:128018. https://doi.org/10.1016/j.biortech.2022.128018
Dong M, He L, Jiang M et al (2023) Biochar for the removal of emerging pollutants from aquatic systems: a review. Int J Environ Res Public Health 20:1679. https://doi.org/10.3390/ijerph20031679
Dou S, Ke X-X, Shao Z-D et al (2022) Fish scale-based biochar with defined pore size and ultrahigh specific surface area for highly efficient adsorption of ciprofloxacin. Chemosphere 287:131962. https://doi.org/10.1016/j.chemosphere.2021.131962
Dzoujo HT, Shikuku VO, Tome S et al (2024) Recent advances in metal oxide-biochar composites for water and soil remediation: a review. Hybrid Adv 7:100292. https://doi.org/10.1016/j.hybadv.2024.100292
Fan M, Li C, Sun Y et al (2021) In situ characterization of functional groups of biochar in pyrolysis of cellulose. Sci Total Environ 799:149354. https://doi.org/10.1016/j.scitotenv.2021.149354
Fernandes MJ, Moreira MM, Paíga P et al (2019) Evaluation of the adsorption potential of biochars prepared from forest and agri-food wastes for the removal of fluoxetine. Bioresour Technol 292:121973. https://doi.org/10.1016/j.biortech.2019.121973
Fu X, Niu X, Zhang D et al (2024) Insights into novel phosphorus-doped biochar for tetracycline removal: non-radical oxidation and adsorption. J Environ Chem Eng 12:114224. https://doi.org/10.1016/j.jece.2024.114224
Ganie ZA, Khandelwal N, Tiwari E et al (2021) Biochar-facilitated remediation of nanoplastic contaminated water: effect of pyrolysis temperature induced surface modifications. J Hazard Mater 417:126096. https://doi.org/10.1016/j.jhazmat.2021.126096
Ghaedi S, Rajabi H, Hadi Mosleh M, Sedighi M (2025) MOF biochar composites for environmental protection and pollution control. Bioresour Technol 418:131982. https://doi.org/10.1016/j.biortech.2024.131982
Gholap V, Subash A, Joseph T, Kandasubramanian B (2025) <scp>2D</scp>-<scp>MXene</scp> composite systems for effective photocatalytic degradation of pharmaceutical compounds. Can J Chem Eng 103:292–310. https://doi.org/10.1002/cjce.25369
Gholipour S, Nikaeen M, Mehdipour M et al (2024) Occurrence of chlorine-resistant Pseudomonas aeruginosa in hospital water systems: threat of waterborne infections for patients. Antimicrob Resist Infect Control 13:111. https://doi.org/10.1186/s13756-024-01468-4
Godlewska P, Jośko I, Oleszczuk P (2022) Ecotoxicity of sewage sludge- or sewage sludge/willow-derived biochar-amended soil. Environ Pollut 305:119235. https://doi.org/10.1016/j.envpol.2022.119235
Gotore O, Itayama T, Dang B-T et al (2024) Adsorption analysis of ciprofloxacin and delafloxacin onto the corn cob derived-biochar under different pyrolysis conditions. Biomass Convers Biorefin 14:10373–10388. https://doi.org/10.1007/s13399-022-03156-y
Greiner BG, Shimabuku KK, Summers RS (2018) Influence of biochar thermal regeneration on sulfamethoxazole and dissolved organic matter adsorption. Environ Sci (Camb) 4:169–174. https://doi.org/10.1039/C7EW00379J
Guo X, Mei N (2014) Assessment of the toxic potential of graphene family nanomaterials. J Food Drug Anal 22:105–115. https://doi.org/10.1016/j.jfda.2014.01.009
Guo D, Shibuya R, Akiba C et al (2016) Active sites of nitrogen-doped carbon materials for oxygen reduction reaction clarified using model catalysts. Science 351:361–365. https://doi.org/10.1126/science.aad0832
Guo W, Huo S, Feng J, Lu X (2017) Adsorption of perfluorooctane sulfonate (PFOS) on corn straw-derived biochar prepared at different pyrolytic temperatures. J Taiwan Inst Chem Eng 78:265–271. https://doi.org/10.1016/j.jtice.2017.06.013
Gupta D, Das A, Mitra S (2023) Role of modeling and artificial intelligence in process parameter optimization of biochar: a review. Bioresour Technol 390:129792. https://doi.org/10.1016/j.biortech.2023.129792
Gwenzi W, Chaukura N, Noubactep C, Mukome FND (2017) Biochar-based water treatment systems as a potential low-cost and sustainable technology for clean water provision. J Environ Manage 197:732–749. https://doi.org/10.1016/j.jenvman.2017.03.087
Han Z, Teah HY, Hirasawa I, Kikuchi Y (2025) Prospective life cycle assessment of emerging silver nanoparticle synthesis methods: one-pot polyethyleneimine chemical reduction and biological reductions. J Clean Prod 494:145012. https://doi.org/10.1016/j.jclepro.2025.145012
Hassan M, Liu Y, Naidu R et al (2020) Adsorption of perfluorooctane sulfonate (PFOS) onto metal oxides modified biochar. Environ Technol Innov 19:100816. https://doi.org/10.1016/j.eti.2020.100816
He Y, Cheng X, Gunjal SJ, Zhang C (2024) Advancing PFAS sorbent design: mechanisms, challenges, and perspectives. ACS Mater Au 4:108–114. https://doi.org/10.1021/acsmaterialsau.3c00066
Heo J, Yoon Y, Lee G et al (2019) Enhanced adsorption of bisphenol A and sulfamethoxazole by a novel magnetic CuZnFe2O4–biochar composite. Bioresour Technol 281:179–187. https://doi.org/10.1016/j.biortech.2019.02.091
Hernandes PT, Franco DSP, Georgin J et al (2022) Investigation of biochar from *Cedrella fissilis* applied to the adsorption of atrazine herbicide from an aqueous medium. J Environ Chem Eng 10:107408. https://doi.org/10.1016/j.jece.2022.107408
Hlongwane GN, Sekoai PT, Meyyappan M, Moothi K (2019) Simultaneous removal of pollutants from water using nanoparticles: a shift from single pollutant control to multiple pollutant control. Sci Total Environ 656:808–833. https://doi.org/10.1016/j.scitotenv.2018.11.257
Hu R, Xiao J, Wang T et al (2020) Engineering of phosphate-functionalized biochars with highly developed surface area and porosity for efficient and selective extraction of uranium. Chem Eng J (Lausanne) 379:122388. https://doi.org/10.1016/j.cej.2019.122388
Hu M, Guo K, Zhou H et al (2024) Techno-economic assessment of swine manure biochar production in large-scale piggeries in China. Energy 308:133037. https://doi.org/10.1016/j.energy.2024.133037
Israel Dikobe P, Tekere M, Masindi V, Foteinis S (2024) Occurrence, persistence, and removal of contaminants of emerging concern through drinking water treatment processes—a case study in South Africa. Environ Nanotechnol Monit Manag 22:100997. https://doi.org/10.1016/j.enmm.2024.100997
Jaria G, Calisto V, Esteves VI, Otero M (2022) Overview of relevant economic and environmental aspects of waste-based activated carbons aimed at adsorptive water treatments. J Clean Prod 344:130984. https://doi.org/10.1016/j.jclepro.2022.130984
Jia H, Zhao Y, Deng H et al (2023) Significant contributions of biochar-derived dissolved matters to ecotoxicity to earthworms (*Eisenia fetida*) in soil with biochar amendment. Environ Technol Innov 29:102988. https://doi.org/10.1016/j.eti.2022.102988
Jin H (2024) Techno-economic assessment of laser-induced biomass graphene. Master of Science - Sustainable Energy Engineering, KTH, School of Industrial Engineering and Management (ITM), Energy Technology
Karadirek IE, Erkaya O, Ciggin AS (2025) Comparative life cycle assessment of sewage sludge drying by solar and thermal drying technologies. Waste Manag 201:114826. https://doi.org/10.1016/j.wasman.2025.114826
Keller AA, Li W, Floyd Y et al (2024) Elimination of microplastics, PFAS, and PPCPs from biosolids via pyrolysis to produce biochar: feasibility and techno-economic analysis. Sci Total Environ 947:174773. https://doi.org/10.1016/j.scitotenv.2024.174773
Khatami M, Iravani P, Jamalipour Soufi G, Iravani S (2022) MXenes for antimicrobial and antiviral applications: recent advances. Mater Technol 37:1890–1905. https://doi.org/10.1080/10667857.2021.2002587
Kim JK, Shin JH, Lee JS et al (2016) 28-day inhalation toxicity of graphene nanoplatelets in Sprague-Dawley rats. Nanotoxicology 10:891–901. https://doi.org/10.3109/17435390.2015.1133865
Krebsbach S, He J, Adhikari S et al (2023) Mechanistic understanding of perfluorooctane sulfonate (PFOS) sorption by biochars. Chemosphere 330:138661. https://doi.org/10.1016/j.chemosphere.2023.138661
Kumari S, Chowdhry J, Kumar M, Garg MC (2024) Machine learning (ML): an emerging tool to access the production and application of biochar in the treatment of contaminated water and wastewater. Groundw Sustain Dev 26:101243. https://doi.org/10.1016/j.gsd.2024.101243
Lee JK, Jeong AY, Bae J et al (2017) The role of surface functionalization on the pulmonary inflammogenicity and translocation into mediastinal lymph nodes of graphene nanoplatelets in rats. Arch Toxicol 91:667–676. https://doi.org/10.1007/s00204-016-1706-y
Lee J, Kim C, Liu C et al (2023) Ultra-high capacity, multifunctional nanoscale sorbents for PFOA and PFOS treatment. NPJ Clean Water 6:62. https://doi.org/10.1038/s41545-023-00263-9
Leng L, Xiong Q, Yang L et al (2021) An overview on engineering the surface area and porosity of biochar. Sci Total Environ 763:144204. https://doi.org/10.1016/j.scitotenv.2020.144204

Leng L, Yang L, Lei X et al (2022) Machine learning predicting and engineering the yield, N content, and specific surface area of biochar derived from pyrolysis of biomass. Biochar 4:63. https://doi.org/10.1007/s42773-022-00183-w

Leng L, Lei X, Abdullah Al-Dhabi N et al (2024) Machine-learning-aided prediction and engineering of nitrogen-containing functional groups of biochar derived from biomass pyrolysis. Chem Eng J 485:149862. https://doi.org/10.1016/j.cej.2024.149862

Leng L, Zheng H, Shen T et al (2025) Engineering biochar from biomass pyrolysis for effective adsorption of heavy metal: an innovative machine learning approach. Sep Purif Technol 361:131592. https://doi.org/10.1016/j.seppur.2025.131592

Li S, Wang Z, Zhao X et al (2019) Insight into enhanced carbamazepine photodegradation over biochar-based magnetic photocatalyst Fe3O4/BiOBr/BC under visible LED light irradiation. Chem Eng J 360:600–611. https://doi.org/10.1016/j.cej.2018.12.002

Li J, Li X, Da Y et al (2022) Sustainable environmental remediation via biomimetic multifunctional lignocellulosic nano-framework. Nat Commun 13:4368. https://doi.org/10.1038/s41467-022-31881-5

Li C, Xu B, Jin M et al (2023a) Sulfur and nitrogen co-doped biochar activated persulfate to degrade phenolic wastewater: changes in impedance. J Mol Struct 1294:136344. https://doi.org/10.1016/j.molstruc.2023.136344

Li H, Ai Z, Yang L et al (2023b) Machine learning assisted predicting and engineering specific surface area and total pore volume of biochar. Bioresour Technol 369:128417. https://doi.org/10.1016/j.biortech.2022.128417

Li Y, Wang B, Shang H et al (2023c) Influence of adsorption sites of biochar on its adsorption performance for sulfamethoxazole. Chemosphere 326:138408. https://doi.org/10.1016/j.chemosphere.2023.138408

Li J, Sun W, Lichtfouse E et al (2024a) Life cycle assessment of biochar for sustainable agricultural application: a review. Sci Total Environ 951:175448. https://doi.org/10.1016/j.scitotenv.2024.175448

Li K, Xu W, Song H et al (2024b) Superior reduction and immobilization of Cr(VI) in soil utilizing sulfide nanoscale zero-valent iron supported by phosphoric acid-modified biochar: efficiency and mechanism investigation. Sci Total Environ 907:168133. https://doi.org/10.1016/j.scitotenv.2023.168133

Li X, Cen K, Wang L et al (2024c) Co-pyrolysis of cellulose and lignin: effects of pyrolysis temperature, residence time, and lignin percentage on the properties of biochar using response surface methodology. Ind Crops Prod 219:119071. https://doi.org/10.1016/j.indcrop.2024.119071

Li X, Shen X, Jiang W et al (2024d) Comprehensive review of emerging contaminants: detection technologies, environmental impact, and management strategies. Ecotoxicol Environ Saf 278:116420. https://doi.org/10.1016/j.ecoenv.2024.116420

Li Y, Zhu Y, Liu J et al (2025a) Review of modified biochar for removing humic acid from water: analysis of structure-activity relationship. Biochar 7:1. https://doi.org/10.1007/s42773-024-00387-2

Li Z, Tong W, Li C et al (2025b) Advances on nitrogen-doped biochar for adsorption and degradation of organic pollutants from aquatic environment: mechanisms and applications. Sep Purif Technol 354:129017. https://doi.org/10.1016/j.seppur.2024.129017

Liang G, Hu Z, Wang Z et al (2020) Effective removal of carbamazepine and diclofenac by CuO/Cu2O/Cu-biochar composite with different adsorption mechanisms. Environ Sci Pollut Res Int 27:45435–45446. https://doi.org/10.1007/s11356-020-10284-3

Liang Y, Tao R, Zhao B et al (2024) Roles of iron and manganese in bimetallic biochar composites for efficient persulfate activation and atrazine removal. Biochar 6:41. https://doi.org/10.1007/s42773-024-00331-4

Lin H, Lao J-Y, Wang Q et al (2022) Per- and polyfluoroalkyl substances in the atmosphere of waste management infrastructures: uncovering secondary fluorotelomer alcohols, particle size distribution, and human inhalation exposure. Environ Int 167:107434. https://doi.org/10.1016/j.envint.2022.107434

Liu J, Yang X, Liu H et al (2021) Mixed biochar obtained by the co-pyrolysis of shrimp shell with corn straw: co-pyrolysis characteristics and its adsorption capability. Chemosphere 282:131116. https://doi.org/10.1016/j.chemosphere.2021.131116

Liu Z, Xu Z, Xu L et al (2022) Modified biochar: synthesis and mechanism for removal of environmental heavy metals. Carbon Res 1:8. https://doi.org/10.1007/s44246-022-00007-3

Liu C, Balasubramanian P, An J, Li F (2025a) Machine learning prediction of ammonia nitrogen adsorption on biochar with model evaluation and optimization. NPJ Clean Water 8:13. https://doi.org/10.1038/s41545-024-00429-z

Liu M, Tao J, Mu L et al (2025b) Machine learning-driven predictions of biochar yield and NPK composition: insights into biomass pyrolysis with data augmentation and model interpretability. Carbon Res 4:62. https://doi.org/10.1007/s44246-025-00229-1

Liu Z, He C, Yang G et al (2025c) Wood powder-derived porous carbon materials synthesis by highly efficient microwave-induced carbothermal shock in molten salts for dye removal. Sustain Mater Technol 45:e01596. https://doi.org/10.1016/j.susmat.2025.e01596

Liyanage AS, Canaday S, Pittman CU, Mlsna T (2020) Rapid remediation of pharmaceuticals from wastewater using magnetic Fe3O4/Douglas fir biochar adsorbents. Chemosphere 258:127336. https://doi.org/10.1016/j.chemosphere.2020.127336

Lu M, Liu Y, Zheng X et al (2024) Amino group-driven adsorption of sodium p-perfluorous nonenoxybenzene sulfonate in water by the modified graphene oxide. Toxics 12:343. https://doi.org/10.3390/toxics12050343

Lyu H, Gao B, He F et al (2018) Effects of ball milling on the physicochemical and sorptive properties of biochar: experimental observations and governing mechanisms. Environ Pollut 233:54–63. https://doi.org/10.1016/j.envpol.2017.10.037

Ma Z, Yang Y, Wu Y et al (2019) In-depth comparison of the physicochemical characteristics of bio-char derived from biomass pseudo components: hemicellulose, cellulose, and lignin. J Anal Appl Pyrolysis 140:195–204. https://doi.org/10.1016/j.jaap.2019.03.015

Ma Y, Wu L, Li P et al (2021) A novel, efficient and sustainable magnetic sludge biochar modified by graphene oxide for environmental concentration imidacloprid removal. J Hazard Mater 407:124777. https://doi.org/10.1016/j.jhazmat.2020.124777

Ma K, Lu Y, Zhang Y, Zhang Y (2024a) Trend of PFAS concentrations and prediction of potential risks in Taihu Lake of China by AQUATOX. Environ Res 251:118707. https://doi.org/10.1016/j.envres.2024.118707

Ma Y, Yao Y, Deng Z et al (2024b) Hydrothermal N-doping, magnetization and ball milling co-functionalized sludge biochar design and its selective adsorption of trace concentration sulfamethoxazole from waters. Chemosphere 363:142855. https://doi.org/10.1016/j.chemosphere.2024.142855

Machado LMM, Perondi D, Manera C et al (2025) Bleached cellulose biochars as a sustainable alternative for oilfield-produced water (OPW) treatment and environmental remediation. Sep Purif Technol 357:130136. https://doi.org/10.1016/j.seppur.2024.130136

Mariyam S, Alherbawi M, McKay G, Al-Ansari T (2025) A predictive model for biomass waste pyrolysis yield: exploring the correlation of proximate analysis and product composition. Energy Convers Manag: X 25:100831. https://doi.org/10.1016/j.ecmx.2024.100831

Marsh H, Rodriguez-Reinoso F (2012) Activated carbon, 1st edn. Elsevier, Oxford

Mašek O, Buss W, Roy-Poirier A et al (2018) Consistency of biochar properties over time and production scales: a characterisation of standard materials. J Anal Appl Pyrolysis 132:200–210. https://doi.org/10.1016/j.jaap.2018.02.020

Masuku M, Ouma L, Pholosi A (2021) Microwave assisted synthesis of oleic acid modified magnetite nanoparticles for benzene adsorption. Environ Nanotechnol Monit Manag 15:100429. https://doi.org/10.1016/j.enmm.2021.100429

Meramo SI, Bonfante H, De Avila-Montiel G et al (2018) Environmental assessment of a large-scale production of TiO2 nanoparticles via green chemistry. Chem Eng Trans 70:1063–1068. https://doi.org/10.3303/CET1870178

Meramo-Hurtado SI, González-Delgado ÁD (2020) Application of techno-economic and sensitivity analyses as decision-making tools for assessing emerging large-scale technologies for production of chitosan-based adsorbents. ACS Omega 5:17601–17610. https://doi.org/10.1021/acsomega.0c02064

Min KH, Kim KH, Seo J-H, Pack SP (2025) Biochar utilization in antimicrobial, anticancer, and biosensing applications: a review. Biomolecules 15:760. https://doi.org/10.3390/biom15060760

Miranda C, Scalera F, Piancastelli A et al (2024) Exploring the potential of a waste-derived bone char for pharmaceuticals adsorption in

saline-based wastewater. Sustain Chem Pharm 42:101761. https://doi.org/10.1016/j.scp.2024.101761
Mishra K, Siwal SS, Sithole T et al (2024) Biorenewable materials for water remediation: the central role of cellulose in achieving sustainability. J Bioresour Bioprod 9:253–282. https://doi.org/10.1016/j.jobab.2023.12.002
Módenes AN, Bazarin G, Borba CE et al (2021) Tetracycline adsorption by tilapia fish bone-based biochar: mass transfer assessment and fixed-bed data prediction by hybrid statistical-phenomenological modeling. J Clean Prod 279:123775. https://doi.org/10.1016/j.jclepro.2020.123775
Mohammadi A, Cowie AL, Anh Mai TL et al (2017) Climate-change and health effects of using rice husk for biochar-compost: comparing three pyrolysis systems. J Clean Prod 162:260–272. https://doi.org/10.1016/j.jclepro.2017.06.026
Mohan D, Sharma R, Singh VK et al (2012) Fluoride removal from water using bio-char, a green waste, low-cost adsorbent: equilibrium uptake and sorption dynamics modeling. Ind Eng Chem Res 51:900–914. https://doi.org/10.1021/ie202189v
Mpongwana N, Rathilal S (2022) A review of the techno-economic feasibility of nanoparticle application for wastewater treatment. Water (Basel) 14:1550. https://doi.org/10.3390/w14101550
Muambo KE, Kim M-G, Kim D-H et al (2024) Pharmaceuticals in raw and treated water from drinking water treatment plants nationwide: insights into their sources and exposure risk assessment. Water Res X 24:100256. https://doi.org/10.1016/j.wroa.2024.100256
Musegades LJ, Curtin OP, Cyran JD (2024) Determining the surface p K a of perfluorooctanoic acid. J Phys Chem C 128:1946–1951. https://doi.org/10.1021/acs.jpcc.3c07235
Narain Singh D, Pandey P, Shankar Singh V, Kumar Tripathi A (2025) Evidence for high-risk pollutants and emerging microbial contaminants at two major bathing ghats of the river Ganga using high-resolution mass spectrometry and metagenomics. Gene 933:148991. https://doi.org/10.1016/j.gene.2024.148991
Ndoun MC, Elliott HA, Preisendanz HE et al (2021) Adsorption of pharmaceuticals from aqueous solutions using biochar derived from cotton gin waste and guayule bagasse. Biochar 3:89–104. https://doi.org/10.1007/s42773-020-00070-2
Negro V, Ruggeri B, Fino D, Tonini D (2017) Life cycle assessment of orange peel waste management. Resour Conserv Recycl 127:148–158. https://doi.org/10.1016/j.resconrec.2017.08.014
Nidheesh PV, Ganiyu SO, Thiam A (2024) Application of biochar in electro-Fenton process: advantages and recent advancements. J Environ Chem Eng 12:112726. https://doi.org/10.1016/j.jece.2024.112726
Noman E, Al-Gheethi A, Talip BA et al (2019) Inactivating pathogenic bacteria in greywater by biosynthesized Cu/Zn nanoparticles from secondary metabolite of *Aspergillus iizukae*; optimization, mechanism and techno economic analysis. PLoS ONE 14:e0221522. https://doi.org/10.1371/journal.pone.0221522
Ocampo-Perez R, Padilla-Ortega E, Medellin-Castillo NA et al (2019) Synthesis of biochar from chili seeds and its application to remove ibuprofen from water. Equilibrium and 3D modeling. Sci Total Environ 655:1397–1408. https://doi.org/10.1016/j.scitotenv.2018.11.283
Olawade DB, Wada OZ, Egbewole BI et al (2024a) Metal and metal oxide nanomaterials for heavy metal remediation: novel approaches for selective, regenerative, and scalable water treatment. Front Nanotechnol. https://doi.org/10.3389/fnano.2024.1466721
Olawade DB, Wada OZ, Fapohunda O et al (2024b) Nanoparticles for microbial control in water: mechanisms, applications, and ecological implications. Front Nanotechnol. https://doi.org/10.3389/fnano.2024.1427843
Oleszczuk P, Pan B, Xing B (2009) Adsorption and desorption of oxytetracycline and carbamazepine by multiwalled carbon nanotubes. Environ Sci Technol 43:9167–9173. https://doi.org/10.1021/es901928q
Oleszczuk P, Jośko I, Kuśmierz M (2013) Biochar properties regarding to contaminants content and ecotoxicological assessment. J Hazard Mater 260:375–382. https://doi.org/10.1016/j.jhazmat.2013.05.044
Olubusoye BS, Cizdziel JV, Wontor K et al (2024) Removal of microplastics from agricultural runoff using biochar: a column feasibility study. Front Environ Sci. https://doi.org/10.3389/fenvs.2024.1388606
Pan X, Gu Z, Chen W, Li Q (2021) Preparation of biochar and biochar composites and their application in a Fenton-like process for wastewater decontamination: a review. Sci Total Environ 754:142104. https://doi.org/10.1016/j.scitotenv.2020.142104
Pandit NR, Mulder J, Hale SE et al (2018) Multi-year double cropping biochar field trials in Nepal: finding the optimal biochar dose through agronomic trials and cost-benefit analysis. Sci Total Environ 637:1333–1341. https://doi.org/10.1016/j.scitotenv.2018.05.107
Pandit S, Yadav N, Sharma P et al (2025) Life cycle assessment and techno-economic analysis of nanotechnology-based wastewater treatment: status, challenges and future prospectives. J Taiwan Inst Chem Eng 166:105567. https://doi.org/10.1016/j.jtice.2024.105567
Peng P, Jiang HZH, Collins S et al (2024) Long duration energy storage using hydrogen in metal-organic frameworks: opportunities and challenges. ACS Energy Lett 9:2727–2735. https://doi.org/10.1021/acsenergylett.4c00894
Peng Q, Ye L, Wen N et al (2025) Nitrogen vacancy-modified g-C3N4 nanosheets controlled by deep eutectic solvents for highly efficient photocatalytic atrazine degradation: non-radical dominated holes oxidation. Sep Purif Technol 354:128879. https://doi.org/10.1016/j.seppur.2024.128879
Piccirillo C, Moreira IS, Novais RM et al (2017) Biphasic apatite-carbon materials derived from pyrolysed fish bones for effective adsorption of persistent pollutants and heavy metals. J Environ Chem Eng 5:4884–4894. https://doi.org/10.1016/j.jece.2017.09.010
Puchana-Rosero MJ, Adebayo MA, Lima EC et al (2016) Microwave-assisted activated carbon obtained from the sludge of tannery-treatment effluent plant for removal of leather dyes. Colloids Surf A Physicochem Eng Asp 504:105–115. https://doi.org/10.1016/j.colsurfa.2016.05.059
Puga A, Moreira MM, Figueiredo SA et al (2021) Electro-Fenton degradation of a ternary pharmaceutical mixture and its application in the regeneration of spent biochar. J Electroanal Chem 886:115135. https://doi.org/10.1016/j.jelechem.2021.115135
Qin J, Ji R, Sun Q et al (2023) Self-activation of potassium/iron citrate-assisted production of porous carbon/porous biochar composites from macroalgae for high-performance sorption of sulfamethoxazole. Bioresour Technol 369:128361. https://doi.org/10.1016/j.biortech.2022.128361
Qu J, Wang S, Jin L et al (2021) Magnetic porous biochar with high specific surface area derived from microwave-assisted hydrothermal and pyrolysis treatments of water hyacinth for Cr(VI) and tetracycline adsorption from water. Bioresour Technol 340:125692. https://doi.org/10.1016/j.biortech.2021.125692
RajabiHamedani S, Kuppens T, Malina R et al (2019) Life cycle assessment and environmental valuation of biochar production: two case studies in Belgium. Energies (Basel) 12:2166. https://doi.org/10.3390/en12112166
Rajapaksha AU, Vithanage M, Lee SS et al (2016) Steam activation of biochars facilitates kinetics and pH-resilience of sulfamethazine sorption. J Soils Sediments 16:889–895. https://doi.org/10.1007/s11368-015-1325-x
Rasheed PA, Rasool K, Younes N et al (2024) Ecotoxicity and environmental safety assessment of two-dimensional niobium carbides (MXenes). Sci Total Environ 947:174563. https://doi.org/10.1016/j.scitotenv.2024.174563
Regkouzas P, Diamadopoulos E (2019) Adsorption of selected organic micropollutants on sewage sludge biochar. Chemosphere 224:840–851. https://doi.org/10.1016/j.chemosphere.2019.02.165
Ren X, Zhang C, Zhang X et al (2025) MOF-derived Fe-Cu doped biochar composites for synchronous adsorption, electro-Fenton oxidation and in-situ regeneration for efficient antibiotic removal. Water Res 287:124408. https://doi.org/10.1016/j.watres.2025.124408
Reynel-Avila HE, Mendoza-Castillo DI, Bonilla-Petriciolet A, Silvestre-Albero J (2015) Assessment of naproxen adsorption on bone char in aqueous solutions using batch and fixed-bed processes. J Mol Liq 209:187–195. https://doi.org/10.1016/j.molliq.2015.05.013
Rikta SY (2019) Application of nanoparticles for disinfection and microbial control of water and wastewater. In: Nanotechnology in water and wastewater treatment. Elsevier, pp 159–176
Rodrigo PM, Navarathna C, Pham MTH et al (2022) Batch and fixed bed sorption of low to moderate concentrations of aqueous per- and poly-fluoroalkyl substances (PFAS) on Douglas fir biochar and its Fe3O4 hybrids. Chemosphere 308:136155. https://doi.org/10.1016/j.chemosphere.2022.136155

Rodríguez-Rojas MdelP, Bustos-Terrones V, Díaz-Cárdenas MY et al (2024) Life cycle assessment of green synthesis of TiO2 nanoparticles vs. chemical synthesis. Sustainability 16:7751. https://doi.org/10.3390/su16177751
Saawarn B, Mahanty B, Hait S (2024) Adsorptive removal of perfluorooctanoic acid from aqueous matrices using peanut husk-derived magnetic biochar: statistical and artificial intelligence approaches, kinetics, isotherm, and thermodynamics. Chemosphere 360:142397. https://doi.org/10.1016/j.chemosphere.2024.142397
Sait HH, Kanthasamy R, Ayodele BV (2025) Hybrid analysis of biochar production from pyrolysis of agriculture waste using statistical and artificial intelligent-based modeling techniques. Agronomy 15:181. https://doi.org/10.3390/agronomy15010181
Salgado MAH, Tarelho LAC, Matos A, et al (2018) Thermoeconomic analysis of integrated production of biochar and process heat from quinoa and lupin residual biomass. Energy Policy 114:332–341. https://doi.org/10.1016/j.enpol.2017.12.014
Samuel Olugbenga O, Goodness Adeleye P, Blessing Oladipupo S et al (2024) Biomass-derived biochar in wastewater treatment- a circular economy approach. Waste Manag Bull 1:1–14. https://doi.org/10.1016/j.wmb.2023.07.007
Satyam S, Patra S (2024) Innovations and challenges in adsorption-based wastewater remediation: a comprehensive review. Heliyon 10:e29573. https://doi.org/10.1016/j.heliyon.2024.e29573
Schlich K, Hoppe M, Kraas M et al (2018) Long-term effects of three different silver sulfide nanomaterials, silver nitrate and bulk silver sulfide on soil microorganisms and plants. Environ Pollut 242:1850–1859. https://doi.org/10.1016/j.envpol.2018.07.082
Severy MA, Carter DJ, Palmer KD et al (2018) Performance and emissions control of commercial-scale biochar production unit. Appl Eng Agric 34:73–84. https://doi.org/10.13031/aea.12375
Sevilla M, Díez N, Fuertes AB (2021) More sustainable chemical activation strategies for the production of porous carbons. Chemsuschem 14:94–117. https://doi.org/10.1002/cssc.202001838
Shah HH, Amin M, Pepe F et al (2023) Overview of environmental and economic viability of activated carbons derived from waste biomass for adsorptive water treatment applications. Environ Sci Pollut Res. https://doi.org/10.1007/s11356-023-30540-6
Shaheen J, Fseha YH, Sizirici B (2022) Performance, life cycle assessment, and economic comparison between date palm waste biochar and activated carbon derived from woody biomass. Heliyon 8:e12388. https://doi.org/10.1016/j.heliyon.2022.e12388
Shaheen SM, Ullah H, Wu Y et al (2025) Remediation of emerging inorganic contaminants in soils and water using pristine and engineered biochar: a review. Biochar 7:34. https://doi.org/10.1007/s42773-024-00407-1
Shanmughan B, Nighojkar A, Kandsubramanian B (2025) Advancements in characterization techniques, empirical models, and artificial intelligence for comprehensive understanding of heavy metal adsorption on sewage sludge biochar. Waste Manag Bull 3:193–206. https://doi.org/10.1016/j.wmb.2025.01.003
Shi D, Yek PNY, Ge S et al (2022a) Production of highly porous biochar via microwave physiochemical activation for dechlorination in water treatment. Chemosphere 309:136624. https://doi.org/10.1016/j.chemosphere.2022.136624
Shi W, Wang H, Yan J et al (2022b) Wheat straw derived biochar with hierarchically porous structure for bisphenol A removal: preparation, characterization, and adsorption properties. Sep Purif Technol 289:120796. https://doi.org/10.1016/j.seppur.2022.120796
Shin JH, Han SG, Kim JK et al (2015) 5-day repeated inhalation and 28-day post-exposure study of graphene. Nanotoxicology 9:1023–1031. https://doi.org/10.3109/17435390.2014.998306
Siipola V, Pflugmacher S, Romar H et al (2020) Low-cost biochar adsorbents for water purification including microplastics removal. Appl Sci 10:788. https://doi.org/10.3390/app10030788
Singh A, Prasad SM, Singh S (2018) Impact of nano ZnO on metabolic attributes and fluorescence kinetics of rice seedlings. Environ Nanotechnol Monit Manag 9:42–49. https://doi.org/10.1016/j.enmm.2017.11.006
Singh N, Khandelwal N, Ganie ZA et al (2021a) Eco-friendly magnetic biochar: an effective trap for nanoplastics of varying surface functionality and size in the aqueous environment. Chem Eng J 418:129405. https://doi.org/10.1016/j.cej.2021.129405
Singh V, Chakravarthi MH, Srivastava VC (2021b) Chemically modified biochar derived from effluent treatment plant sludge of a distillery for the removal of an emerging pollutant, tetracycline, from aqueous solution. Biomass Convers Biorefin 11:2735–2746. https://doi.org/10.1007/s13399-020-00683-4
Singh G, Thakur N, Kumar R (2024) Nanoparticles in drinking water: assessing health risks and regulatory challenges. Sci Total Environ 949:174940. https://doi.org/10.1016/j.scitotenv.2024.174940
Skjennum KA, Krahn KM, Sørmo E et al (2024) The impact of biochar's physicochemical properties on sorption of perfluorooctanoic acid (PFOA). Sci Total Environ 955:177191. https://doi.org/10.1016/j.scitotenv.2024.177191
Smaili H, Ng C (2023) Adsorption as a remediation technology for short-chain per- and polyfluoroalkyl substances (PFAS) from water—a critical review. Environ Sci (Camb) 9:344–362. https://doi.org/10.1039/D2EW00721E
Song L, Cheng H, Liu C et al (2024) Oyster shell facilitates the green production of nitrogen-doped porous biochar from macroalgae: a case study for removing atrazine from water. Biochar 6:76. https://doi.org/10.1007/s42773-024-00372-9
Soriano Y, Carmona E, Renovell J et al (2024) Co-occurrence and spatial distribution of organic micropollutants in surface waters of the River Aconcagua and Maipo basins in Central Chile. Sci Total Environ 954:176314. https://doi.org/10.1016/j.scitotenv.2024.176314
Sui L, Guo H, Yang Y-Y et al (2025) Surface electric fields-enhanced biochar: a dual-action adsorbent and PMS activator for sulfamethoxazole removal. Sep Purif Technol 358:130370. https://doi.org/10.1016/j.seppur.2024.130370
Sun C, Wang Z, Chen L, Li F (2020) Fabrication of robust and compressive chitin and graphene oxide sponges for removal of microplastics with different functional groups. Chem Eng J 393:124796. https://doi.org/10.1016/j.cej.2020.124796
Sun K, Yang W, Shen Y et al (2025a) Green solid-state synthesis of Cu4O3/biochar composites with high antimicrobial activity. Green Chem 27:1462–1474. https://doi.org/10.1039/D4GC04616A
Sun X, Hu Y, Chen M et al (2025b) Improved mercury removal performance and leaching stability of Fe/Br co-doped biochars synthesized through one-step pyrolysis. Fuel 381:133425. https://doi.org/10.1016/j.fuel.2024.133425
Supraja KV, Kachroo H, Viswanathan G et al (2023) Biochar production and its environmental applications: recent developments and machine learning insights. Bioresour Technol 387:129634. https://doi.org/10.1016/j.biortech.2023.129634
Taghavi SM, Momenpour M, Azarian M et al (2013) Effects of nanoparticles on the environment and outdoor workplaces. Electron Phys 5:706–712. https://doi.org/10.14661/2013.706-712
Tan G, Sun W, Xu Y et al (2016) Sorption of mercury (II) and atrazine by biochar, modified biochars and biochar based activated carbon in aqueous solution. Bioresour Technol 211:727–735. https://doi.org/10.1016/j.biortech.2016.03.147
Tan X, Zhong J, Fu C et al (2021) Amphiphilic perfluoropolyether copolymers for the effective removal of polyfluoroalkyl substances from aqueous environments. Macromolecules 54:3447–3457. https://doi.org/10.1021/acs.macromol.1c00096
Tang Y, Zhang S, Su Y et al (2021) Removal of microplastics from aqueous solutions by magnetic carbon nanotubes. Chem Eng J 406:126804. https://doi.org/10.1016/j.cej.2020.126804
Temizel-Sekeryan S, Hicks AL (2020) Global environmental impacts of silver nanoparticle production methods supported by life cycle assessment. Resour Conserv Recycl 156:104676. https://doi.org/10.1016/j.resconrec.2019.104676
Toles CA, Marshall WE, Johns MM et al (2000a) Acid-activated carbons from almond shells: physical, chemical and adsorptive properties and estimated cost of production. Bioresour Technol 71:87–92. https://doi.org/10.1016/S0960-8524(99)00029-2
Toles CA, Marshall WE, Wartelle LH, McAloon A (2000b) Steam- or carbon dioxide-activated carbons from almond shells: physical, chemical and adsorptive properties and estimated cost of production. Bioresour Technol 75:197–203. https://doi.org/10.1016/S0960-8524(00)00058-4
Tong M, He L, Rong H et al (2020) Transport behaviors of plastic particles in saturated quartz sand without and with biochar/Fe3O4-biochar

amendment. Water Res 169:115284. https://doi.org/10.1016/j.watres.2019.115284
Ullah H, Khan S, Zhu X et al (2025) Machine learning-aided biochar design for the adsorptive removal of emerging inorganic pollutants in water. Sep Purif Technol 362:131421. https://doi.org/10.1016/j.seppur.2025.131421
USEPA (2017) Technical fact sheet—perfluorooctane sulfonate (PFOS) and perfluorooctanoic acid (PFOA). Washington
Varela CF, Moreno-Aldana LC, Agámez-Pertuz YY (2024) Adsorption of pharmaceutical pollutants on ZnCl2-activated biochar from corn cob: efficiency, selectivity and mechanism. J Bioresour Bioprod 9:58–73. https://doi.org/10.1016/j.jobab.2023.10.003
Vasiljevic T, Harner T (2021) Bisphenol A and its analogues in outdoor and indoor air: properties, sources and global levels. Sci Total Environ 789:148013. https://doi.org/10.1016/j.scitotenv.2021.148013
Wada OZ, Olawade DB (2025) Recent occurrence of pharmaceuticals in freshwater, emerging treatment technologies, and future considerations: a review. Chemosphere 374:144153. https://doi.org/10.1016/j.chemosphere.2025.144153
Wang S, Zhao X, Xing G, Yang L (2013) Large-scale biochar production from crop residue: a new idea and the biogas-energy pyrolysis system. BioResources 8:8–11
Wang Y, Lu J, Wu J et al (2015) Adsorptive removal of fluoroquinolone antibiotics using bamboo biochar. Sustainability 7:12947–12957. https://doi.org/10.3390/su70912947
Wang Z, Sedighi M, Lea-Langton A (2020) Filtration of microplastic spheres by biochar: removal efficiency and immobilisation mechanisms. Water Res 184:116165. https://doi.org/10.1016/j.watres.2020.116165
Wang J, Sun C, Huang Q-X et al (2021) Adsorption and thermal degradation of microplastics from aqueous solutions by Mg/Zn modified magnetic biochars. J Hazard Mater 419:126486. https://doi.org/10.1016/j.jhazmat.2021.126486
Wang S, Meng X, Yan X et al (2023) Iron and nitrogen modified sludge biochar efficiently activated persulfate for mineralization of sulfamethoxazole in groundwater. J Environ Chem Eng 11:111319. https://doi.org/10.1016/j.jece.2023.111319
Wang H, Yang Y, Wang M et al (2024) Insights into the roles of surface functional groups and micropores in the sorption of ofloxacin on banana pseudo-stem biochars. Sustainability 16:2629. https://doi.org/10.3390/su16072629
Wang H, Zhang H, He L et al (2025a) Environmental behavior of per- and polyfluoroalkyl substances (PFASs) and the potential role of biochar for its remediation: a review. Biochar 7:14. https://doi.org/10.1007/s42773-024-00410-6
Wang S, Song X, Duan J et al (2025b) Automated machine learning-based prediction of the effects of physicochemical properties and external experimental conditions on cadmium adsorption by biochar. Water 17:2266. https://doi.org/10.3390/w17152266
Wątor K, Rusiniak P, Kmiecik E et al (2024) Assessing health risks in bottled water: chemical compounds and their impact on human health. Environ Geochem Health 46:178. https://doi.org/10.1007/s10653-024-01908-5
Wu J, Lu J, Zhang C et al (2019) Adsorptive removal of tetracyclines and fluoroquinolones using Yak dung biochar. Bull Environ Contam Toxicol 102:407–412. https://doi.org/10.1007/s00128-018-2516-0
Wurzer C, Masek O, Oesterie P, Jansson S (2019) Designing activated mineral biochar composites for the adsorption and degradation of emerging contaminants. In: Berruti F, Chiaramonti D, Masek O, Garcia-Perez M (eds) Bio-char ii: production, characterization and applications. ECI Digital Archives, Calabria
Wurzer C, Oesterle P, Jansson S, Masek O (2020) A parallel optimisation of adsorption and regeneration properties of activated biochars for wastewater treatment. In: 22nd EGU General Assembly
Xia X, Zeng S, Li K et al (2025) Unraveling the outstanding catalytic efficiency of unprocessed bone-derived biochar: a deep dive into the mechanisms of native organic encapsulation and defective nitrogen doping in boosting persulfate activation for tetracycline degradation. Sep Purif Technol 353:128571. https://doi.org/10.1016/j.seppur.2024.128571
Xiang L, Liu S, Ye S et al (2021) Potential hazards of biochar: the negative environmental impacts of biochar applications. J Hazard Mater 420:126611. https://doi.org/10.1016/j.jhazmat.2021.126611
Xie G, Zhu C, Li C et al (2025) Predicting the adsorption of ammonia nitrogen by biochar in water bodies using machine learning strategies: model optimization and analysis of key characteristic variables. Environ Res 267:120618. https://doi.org/10.1016/j.envres.2024.120618
Xu Y, Deng F, Pang Q et al (2018) Development of waste-derived sorbents from biomass and brominated flame retarded plastic for elemental mercury removal from coal-fired flue gas. Chem Eng J 350:911–919. https://doi.org/10.1016/j.cej.2018.06.055
Xue Y, Guo Y, Zhang X et al (2022) Efficient adsorptive removal of ciprofloxacin and carbamazepine using modified pinewood biochar—a kinetic, mechanistic study. Chem Eng J 450:137896. https://doi.org/10.1016/j.cej.2022.137896
Yan J, Zuo X, Yang S et al (2022) Evaluation of potassium ferrate activated biochar for the simultaneous adsorption of copper and sulfadiazine: competitive versus synergistic. J Hazard Mater 424:127435. https://doi.org/10.1016/j.jhazmat.2021.127435
Yang F, Gao Y, Sun L et al (2018) Effective sorption of atrazine by biochar colloids and residues derived from different pyrolysis temperatures. Environ Sci Pollut Res Int 25:18528–18539. https://doi.org/10.1007/s11356-018-2077-0
Yang Q, Mašek O, Zhao L et al (2021) Country-level potential of carbon sequestration and environmental benefits by utilizing crop residues for biochar implementation. Appl Energy 282:116275. https://doi.org/10.1016/j.apenergy.2020.116275
Yang H, Lee C-G, Lee J (2023) Utilizing animal manure-derived biochar in catalytic advanced oxidation processes: a review. J Water Process Eng 56:104545. https://doi.org/10.1016/j.jwpe.2023.104545
Yang H, Han M, Zhang W et al (2024) High performance mixed-dimensional assembled MXene composite membranes for molecular sieving. J Membr Sci 698:122606. https://doi.org/10.1016/j.memsci.2024.122606
Yang Y, Li G, Yue X et al (2025a) Advances in biochar composites for environmental sustainability. Adv Compos Hybrid Mater 8:74. https://doi.org/10.1007/s42114-024-01181-1
Yang Y, Liu Z, Zhang Q et al (2025b) Recent advances of high-rate hard carbon anodes for sodium-ion batteries: correlations between performance and microstructure. Adv Funct Mater. https://doi.org/10.1002/adfm.202514132
Yao H, Lu J, Wu J et al (2013) Adsorption of fluoroquinolone antibiotics by wastewater sludge biochar: role of the sludge source. Water Air Soil Pollut 224:1370. https://doi.org/10.1007/s11270-012-1370-7
Yashni G, Al-Gheethi A, Radin Mohamed RMS et al (2021) Bio-inspired ZnO NPs synthesized from *Citrus sinensis* peels extract for Congo red removal from textile wastewater via photocatalysis: optimization, mechanisms, techno-economic analysis. Chemosphere 281:130661. https://doi.org/10.1016/j.chemosphere.2021.130661
Yin W, Zhang Z, Liu T et al (2020) N-doped animal keratin waste porous biochar derived from Trapa natans husks. Materials 13:987. https://doi.org/10.3390/ma13040987
Yu X, Wang L, Shen X et al (2025) New insight into the S and N co-doped poplar biochar for efficient BPA removal via peroxymonosulfate activation: S for adsorptive removal and N for catalytic removal. Sep Purif Technol 354:128809. https://doi.org/10.1016/j.seppur.2024.128809
Zaed MA, Tan KH, Abdullah N et al (2024) Cost analysis of MXene for low-cost production, and pinpointing of its economic footprint. Open Ceram 17:100526. https://doi.org/10.1016/j.oceram.2023.100526
Zaggia A, Conte L, Falletti L et al (2016) Use of strong anion exchange resins for the removal of perfluoroalkylated substances from contaminated drinking water in batch and continuous pilot plants. Water Res 91:137–146. https://doi.org/10.1016/j.watres.2015.12.039
Zhang DQ, Zhang WL, Liang YN (2019) Adsorption of perfluoroalkyl and polyfluoroalkyl substances (PFASs) from aqueous solution - a review. Sci Total Environ 694:133606. https://doi.org/10.1016/j.scitotenv.2019.133606
Zhang W, Sheng X, Yan J et al (2023) The crucial role of different NaOH activation pathways on the algae-derived biochar toward carbamazepine adsorption. Results Eng 20:101509. https://doi.org/10.1016/j.rineng.2023.101509
Zhang M, Liu R, Huang J et al (2025) Life cycle assessment and environmental benefit analysis of a modified biochar system for heavy metal wastewater treatment. J Water Process Eng 76:108072. https://doi.org/10.1016/j.jwpe.2025.108072

Zhao J, Wang Z, White JC, Xing B (2014) Graphene in the aquatic environment: adsorption, dispersion, toxicity and transformation. Environ Sci Technol 48:9995–10009. https://doi.org/10.1021/es5022679

Zhao H, Ma F, Ren X et al (2025) Green synthesis of nZVI-modified sludge biochar for Cr(VI) removal in water: fixed-bed experiments and artificial neural network model prediction. Water 17:341. https://doi.org/10.3390/w17030341

Zhou L, Huang Q, Ji H et al (2023) Efficient adsorption of bisphenol A from water by a hierarchically porous hyper-crosslinked polymer containing β-cyclodextrin polyurethane. Sep Purif Technol 319:124076. https://doi.org/10.1016/j.seppur.2023.124076

Zhou X, Liu X, Sun L et al (2024) Prediction of biochar yield and specific surface area based on integrated learning algorithm. C 10:10. https://doi.org/10.3390/c10010010

Zhu Y, Liu X, Hu Y et al (2019) Behavior, remediation effect and toxicity of nanomaterials in water environments. Environ Res 174:54–60. https://doi.org/10.1016/j.envres.2019.04.014

Zhu X, Labianca C, He M et al (2022) Life-cycle assessment of pyrolysis processes for sustainable production of biochar from agro-residues. Bioresour Technol 360:127601. https://doi.org/10.1016/j.biortech.2022.127601

Zhuang Z, Wang L, Tang J (2021) Efficient removal of volatile organic compound by ball-milled biochars from different preparing conditions. J Hazard Mater 406:124676. https://doi.org/10.1016/j.jhazmat.2020.124676

Zhuang Z, Mohamed BA, Li LY, Swei O (2022) An economic and global warming impact assessment of common sewage sludge treatment processes in North America. J Clean Prod 370:133539. https://doi.org/10.1016/j.jclepro.2022.133539